

# Improved Algorithms for Computing Worst Value-at-Risk: Numerical Challenges and the Adaptive Rearrangement Algorithm

Marius Hofert<sup>1</sup>, Amir Memartoluie<sup>2</sup>, David Saunders<sup>3</sup>, Tony Wirjanto<sup>4</sup>

2022-06-24

## Abstract

Numerical challenges inherent in algorithms for computing worst Value-at-Risk in homogeneous portfolios are identified and words of warning concerning their implementation are raised. Furthermore, both conceptual and computational improvements to the Rearrangement Algorithm for approximating worst Value-at-Risk for portfolios with arbitrary marginal loss distributions are provided. In particular, a novel Adaptive Rearrangement Algorithm is introduced and investigated. These algorithms are implemented using the R package qrmtools.

## Keywords

Risk aggregation, model uncertainty, Rearrangement Algorithm, Value-at-Risk.

## MSC2010

65C60, 62P05

## 1 Introduction

An integral part of Quantitative Risk Management (QRM) is to analyze the one-period ahead vector of losses  $\mathbf{L} = (L_1, \dots, L_d)^\top$ , where  $L_j$  represents the loss (a random variable) associated with a given business line or risk type with counterparty  $j$ ,  $j \in \{1, \dots, d\}$  over a fixed time horizon. Financial institutions often consider the *aggregated loss*

$$L^+ = \sum_{j=1}^d L_j,$$

---

<sup>1</sup>Department of Statistics and Actuarial Science, University of Waterloo, 200 University Avenue West, Waterloo, ON, N2L 3G1, [marius.hofert@uwaterloo.ca](mailto:marius.hofert@uwaterloo.ca)

<sup>2</sup>Cheriton School of Computer Science, University of Waterloo, 200 University Avenue West, Waterloo, ON, N2L 3G1, [amir.memartoluie@uwaterloo.ca](mailto:amir.memartoluie@uwaterloo.ca)

<sup>3</sup>Department of Statistics and Actuarial Science, University of Waterloo, 200 University Avenue West, Waterloo, ON, N2L 3G1, [david.saunders@uwaterloo.ca](mailto:david.saunders@uwaterloo.ca)

<sup>4</sup>Department of Statistics and Actuarial Science, University of Waterloo, 200 University Avenue West, Waterloo, ON, N2L 3G1, [tony.wirjanto@uwaterloo.ca](mailto:tony.wirjanto@uwaterloo.ca)

## 2 Known optimal solutions in the homogeneous case and their computation

of particular interest. Under Pillar I of the Basel Accords, financial institutions are required to set capital to manage market, credit and operational risk. To this end a risk measure  $\rho(\cdot)$  is used to map the aggregate position  $L^+$  to  $\rho(L^+) \in \mathbb{R}$  for obtaining the amount of capital required to account for the losses in a predetermined time period ahead. As a risk measure, Value-at-Risk ( $\text{VaR}_\alpha$ ) has been widely adopted by the financial industry since the mid nineties. It is defined as the  $\alpha$ -quantile of the distribution function  $F_{L^+}$  of  $L^+$ , i.e.,

$$\text{VaR}_\alpha(L^+) = F_{L^+}^-(\alpha) = \inf\{x \in \mathbb{R} : F_{L^+}(x) \geq \alpha\},$$

where  $F_{L^+}^-$  denotes the quantile function of  $F_{L^+}$ ; see Embrechts and Hofert (2013) for more details. A well known drawback of  $\text{VaR}_\alpha(L^+)$  as a risk measure is that  $\text{VaR}_\alpha(L^+)$  is not necessarily subadditive unless  $\mathbf{L}$  follows an elliptical distribution; see, e.g., Embrechts et al. (2009), McNeil et al. (2005, p. 241), Embrechts et al. (2013) and Hofert and McNeil (2014).

There are various methods for estimating the marginal loss distributions  $F_1, \dots, F_d$  of  $L_1, \dots, L_d$ , respectively, but capturing the  $d$ -variate dependence structure (i.e., the copula) of  $\mathbf{L}$  is often more difficult as typically not much is known about the underlying copula  $C$ . In this work we focus on the case where  $C$  is unknown; the case of partial information about  $C$ , is studied by Bernard et al. (2013) and Bernard et al. (2014). In our case, one only knows that  $\text{VaR}_\alpha(L^+) \in [\underline{\text{VaR}}_\alpha(L^+), \overline{\text{VaR}}_\alpha(L^+)]$  where  $\underline{\text{VaR}}_\alpha(L^+)$  and  $\overline{\text{VaR}}_\alpha(L^+)$  denote the best and the worst  $\text{VaR}_\alpha(L^+)$  over all distributions of  $\mathbf{L}$  with marginals  $F_1, \dots, F_d$ , respectively. An analytical solution for  $\text{VaR}_\alpha(L^+)$  (or the best or worst  $\text{VaR}_\alpha$ ) is not available if  $d \geq 3$ .

In this work we investigate the Rearrangement and “explicit” algorithms of Embrechts et al. (2013) and Embrechts et al. (2014) for computing the worst  $\text{VaR}_\alpha$ , so  $\overline{\text{VaR}}_\alpha(L^+)$ , which is of concern to QRM. The presented algorithms have been implemented in the R package `qrmtools` `qrmtools`<sup>5</sup> and `demo(worst_VaR)` provides results for further numerical investigations and conducts diagnostic checks. For a different approach for computing  $\overline{\text{VaR}}_\alpha(L^+)$ , see Bernard and McLeish (2015).

This paper is organized as follows. In Section 2 we highlight numerical challenges that practitioners may face when implementing theoretical solutions for  $\overline{\text{VaR}}_\alpha(L^+)$  in the homogeneous case  $F_1 = \dots = F_d$ . Section 3 presents the main concept underlying the Rearrangement Algorithm (RA) for computing  $(\underline{\text{VaR}}_\alpha(L^+)$  and)  $\overline{\text{VaR}}_\alpha(L^+)$ , levies criticism on its tuning parameters and investigates its empirical performance using various test cases. Section 4 then presents an improved version of the RA coined as the Adaptive Rearrangement Algorithm (ARA), for calculating  $\overline{\text{VaR}}_\alpha(L^+)$ . Section 5 concludes.

## 2 Known optimal solutions in the homogeneous case and their computation

In order to assess the quality of algorithms such as the RA, we need to know (at least some) optimal solutions with which we can compare such algorithms. Embrechts et al.

<sup>5</sup>The package has not been released to CRAN yet but is available on R-Forge.

## 2 Known optimal solutions in the homogeneous case and their computation

(2013, Proposition 4) and Embrechts et al. (2014, Proposition 3.1) present mathematical formulas for obtaining the worst Value-at-Risk  $\overline{\text{VaR}}_\alpha$  in the homogeneous case. In this section, we address numerical aspects and algorithmic improvements for computing  $\overline{\text{VaR}}_\alpha$  in the homogeneous case; for the general case, see Section 4. We assume  $d \geq 3$  throughout; for  $d = 2$ , Embrechts et al. (2013, Proposition 2) provide an explicit solution to this.

### 2.1 Crude bounds for any $\text{VaR}_\alpha(L^+)$

The following lemma provides (crude) bounds for  $\text{VaR}_\alpha(L^+)$ . Such bounds are useful for computing initial intervals and conducting sanity checks. Note that we do not make any (moment or other) assumptions on the involved marginal loss distributions and the bounds do not depend on the underlying unknown copula.

**Lemma 2.1 (Crude bounds for  $\text{VaR}_\alpha(L^+)$ )**

Let  $L_j \sim F_j$ ,  $j \in \{1, \dots, d\}$ . For any  $\alpha \in (0, 1)$ ,

$$d \min_j F_j^-(\alpha/d) \leq \text{VaR}_\alpha(L^+) \leq d \max_j F_j^-\left(\frac{d-1+\alpha}{d}\right), \quad (1)$$

where  $F_j^-$  denotes the quantile function of  $F_j$ , i.e.,  $F_j^-(u) = \inf\{x \in \mathbb{R} : F_j(x) \geq u\}$ .

*Proof.* Consider the lower bound for  $\text{VaR}_\alpha(L^+)$ . By De Morgan's Law and Boole's inequality, the distribution function  $F_{L^+}$  of  $L^+$  satisfies

$$\begin{aligned} F_{L^+}(x) &= \mathbb{P}\left(\sum_{j=1}^d L_j \leq x\right) \leq \mathbb{P}(\min_j L_j \leq x/d) = \mathbb{P}\left(\bigcup_{j=1}^d \{L_j \leq x/d\}\right) \leq \sum_{j=1}^d \mathbb{P}(L_j \leq x/d) \\ &\leq d \max_j F_j(x/d). \end{aligned}$$

Now  $d \max_j F_j(x/d) \leq \alpha$  if and only if  $x \leq d \min_j F_j^-(\alpha/d)$  and thus  $\text{VaR}_\alpha(L^+) = F_{L^+}^-(\alpha) \geq d \min_j F_j^-(\alpha/d)$ .

Similarly, for the upper bound for  $\text{VaR}_\alpha(L^+)$ , we have that

$$\begin{aligned} F_{L^+}(x) &= \mathbb{P}\left(\sum_{j=1}^d L_j \leq x\right) \geq \mathbb{P}(\max_j L_j \leq x/d) = \mathbb{P}(L_1 \leq x/d, \dots, L_d \leq x/d) \\ &= 1 - \mathbb{P}\left(\bigcup_{j=1}^d \{L_j > x/d\}\right) \geq \max\left\{1 - \sum_{j=1}^d \mathbb{P}(L_j > x/d), 0\right\} \\ &= \max\left\{\sum_{j=1}^d F_j(x/d) - d + 1, 0\right\} \geq \max\{d \min_j F_j(x/d) - d + 1, 0\}. \end{aligned}$$

Now  $d \min_j F_j(x/d) - d + 1 \geq \alpha$  if and only if  $x \geq d \max_j F_j^-((d-1+\alpha)/d)$  and thus  $\text{VaR}_\alpha(L^+) = F_{L^+}^-(\alpha) \leq d \max_j F_j^-((d-1+\alpha)/d)$ .  $\square$

## 2 Known optimal solutions in the homogeneous case and their computation

The bounds (1) can be computed with the function `crude_VaR_bounds()` in the R package `qrmtools`.

### 2.2 The dual bound approach for computing $\overline{\text{VaR}}_\alpha(L^+)$

This approach for computing  $\overline{\text{VaR}}_\alpha(L^+)$  in the homogeneous case with margin(s)  $F$  is presented in Embrechts et al. (2013, Proposition 4) and termed the *dual bound approach* in what follows. In the remaining part of this subsection we assume that  $F(0) = 0$ ,  $F(x) < 1$  for all  $x \in [0, \infty)$  and that  $F$  is absolutely continuous with ultimately decreasing density. Let

$$D(s, t) = \frac{d}{s - dt} \int_t^{s-(d-1)t} \bar{F}(x) dx \quad \text{and} \quad D(s) = \min_{t \in [0, s/d]} D(s, t), \quad (2)$$

where  $\bar{F}(x) = 1 - F(x)$ . In comparison to Embrechts et al. (2013, Proposition 4), the *dual bound*  $D$  here uses a compact interval for  $t$  (and thus  $\min\{\cdot\}$ ) by our requirement  $F(0) = 0$  and since  $\lim_{t \uparrow s/d} D(s, t) = d\bar{F}(s/d)$  by l'Hospital's Rule. The procedure for computing  $\overline{\text{VaR}}_\alpha(L^+)$  according to Embrechts et al. (2013, Proposition 4) can now be given as follows.

#### Algorithm 2.2 (Computing $\overline{\text{VaR}}_\alpha(L^+)$ according to the dual bound approach)

- 1) Specify initial intervals  $[s_l, s_u]$  and  $[t_l, t_u]$ .
- 2) Inner root-finding in  $t$ : For each fixed  $s \in [s_l, s_u]$ , compute  $D(s)$  by iterating over  $t \in [t_l, t_u]$  until a  $t^*$  is found for which  $h(s, t^*) = 0$ , where

$$h(s, t) := D(s, t) - (\bar{F}(t) + (d-1)\bar{F}(s - (d-1)t)).$$

Then  $D(s) = \bar{F}(t^*) + (d-1)\bar{F}(s - (d-1)t^*)$ .

- 3) Outer root-finding in  $s$ : Iterate Step 2) over  $s \in [s_l, s_u]$  until an  $s^*$  is found for which  $D(s^*) = 1 - \alpha$ . Then return  $s^* = \overline{\text{VaR}}_\alpha(L^+)$ .

Algorithm 2.2 is implemented in the function `worst_VaR_hom(..., method="dual")` in the R package `qrmtools`; the dual bound  $D$  is available via `dual_bound()`. It essentially requires a one-dimensional numerical integration (`integrate()` in R), unless  $\bar{F}$  can be integrated explicitly, within two nested calls of a root-finding algorithm (`uniroot()` in R). Note that Algorithm 2.2 requires specification of the two initial intervals  $[s_l, s_u]$  and  $[t_l, t_u]$  and Embrechts et al. (2013) give no particular practical advice on how to choose them.

First consider  $[t_l, t_u]$ . By our requirement  $F(0) = 0$  one can choose  $t_l = 0$  (or the infimum of the support of  $F$ ). For  $t_u$  one would like to choose  $s/d$ . However, care has to be taken as  $h(s, s/d) = 0$  for any  $s$  and thus the inner root-finding procedure will directly stop when a root is found at  $t_u = s/d$ . To take care of this, the inner root-finding algorithm in `worst_VaR_hom(..., method="dual")` fixes `f.upper` to a small number of an opposite sign to  $h(s, 0)$  so that it is able to detect a root below  $t_u = s/d$ ; note that this is an adjustment in the function value, and not in the root-finding interval  $[t_l, t_u]$ .

## 2 Known optimal solutions in the homogeneous case and their computation

Now consider  $[s_l, s_u]$ , in particular,  $s_l$ . According to Embrechts et al. (2013, Proposition 4) it has to be chosen “sufficiently large”. If  $s_l$  is chosen too small, the inner root-finding procedure in Step 2) of Algorithm 2.2 will not be able to locate a root; see also the left-hand side of Figure 1. There is currently no (good) solution on how to automatically determine a sufficiently large  $s_l$ . Given  $s_l$ , one can choose  $s_u$  as the maximum of  $s_l + 1$  and the upper bound  $\text{VaR}_\alpha$  as given in (1), for example. We now show a few selected properties of  $D(s, t)$  and  $D(s)$ .

### Proposition 2.3 (Properties of $D(s, t)$ and $D(s)$ )

- 1)  $D(s)$  is decreasing.
- 2) If  $\bar{F}$  is convex, so is  $D(s, t)$ .

*Proof.*

- 1) Let  $s \geq s'$  and  $t' \in [0, \frac{s'}{d}]$  such that  $D(s', t') = D(s')$ . Define

$$t = \frac{s - (s' - t'd)}{d} = \frac{s - s'}{d} + t'$$

so that  $0 \leq t' \leq t \leq \frac{s}{d}$ . Let  $\kappa = s' - t'd = s - td$ . If  $\kappa > 0$ , noting that  $\bar{F}$  is decreasing and that  $t' \leq t$ , we obtain

$$D(s', t') - D(s, t) = \frac{d}{\kappa} \left( \int_{t'}^{t'+\kappa} \bar{F}(x) dx - \int_t^{t+\kappa} \bar{F}(x) dx \right) \geq 0,$$

so that  $D(s) \leq D(s, t) \leq D(s', t') = D(s')$ . If  $\kappa = 0$  then  $D(s') = D(s', \frac{s'}{d}) = d\bar{F}(\frac{s'}{d}) \geq d\bar{F}(\frac{s}{d}) \geq D(s)$ .

- 2) Recall that  $D(s, t) = \frac{d}{s - td} \int_t^{t+(s-td)} \bar{F}(x) dx$ . Using the transformation  $z = (x - t)/(s - td)$ , we have

$$D(s, t) = d \int_0^1 \bar{F}(sz + t(1 - zd)) dz$$

Define  $C = \{(s, t) \mid 0 \leq s < \infty, 0 \leq t \leq \frac{s}{d}\}$ , and note that  $C$  is convex. Furthermore, if  $\bar{F}$  is convex, then  $D(s, t)$  is jointly convex in  $s$  and  $t$  on  $C$  since for  $\lambda \in (0, 1)$ ,

$$\begin{aligned} & D(\lambda s_1 + (1 - \lambda)s_2, \lambda t_1 + (1 - \lambda)t_2) \\ &= d \int_0^1 \bar{F}((\lambda s_1 + (1 - \lambda)s_2)z + (\lambda t_1 + (1 - \lambda)t_2)(1 - zd)) dz \\ &= d \int_0^1 \bar{F}(\lambda(s_1 z + t_1(1 - zd)) + (1 - \lambda)(s_2 z + t_2(1 - zd))) dz \\ &\leq \int_0^1 \lambda \bar{F}((s_1 + t_1(1 - zd))) + (1 - \lambda) \bar{F}((s_2 + t_2(1 - zd))) dz \\ &= \lambda D(s_1, t_1) + (1 - \lambda) D(s_2, t_2) \end{aligned}$$

□

## 2 Known optimal solutions in the homogeneous case and their computation

Proposition 2.3 Part 2) shows that if  $\bar{F}$  is strictly convex, so is  $D(s, \cdot)$  for fixed  $s$ , which gives the uniqueness of the minimum when computing  $D(s)$  as in (2). A standard result on convexity of marginal value functions then implies that  $D(s)$  is convex; see Rockafellar and Wets (1998, Proposition 2.22).

### Example 2.4 (Auxiliary functions for the dual bound approach)

As an example, consider  $d = 8$  Par( $\theta$ ) risks,  $\theta > 0$ . The left-hand side of Figure 1 illustrates  $t \mapsto h(s, t)$  for  $\theta = 2$  and various  $s$ . Note that  $h(s, s/d)$  is indeed 0 and for (too) small  $s$ ,  $h(s, t)$  does not have a root for  $t \in [0, s/d]$  as mentioned above. The right-hand side of Figure 1 shows the decreasing dual bound  $D(s)$  for various parameters  $\theta$ .

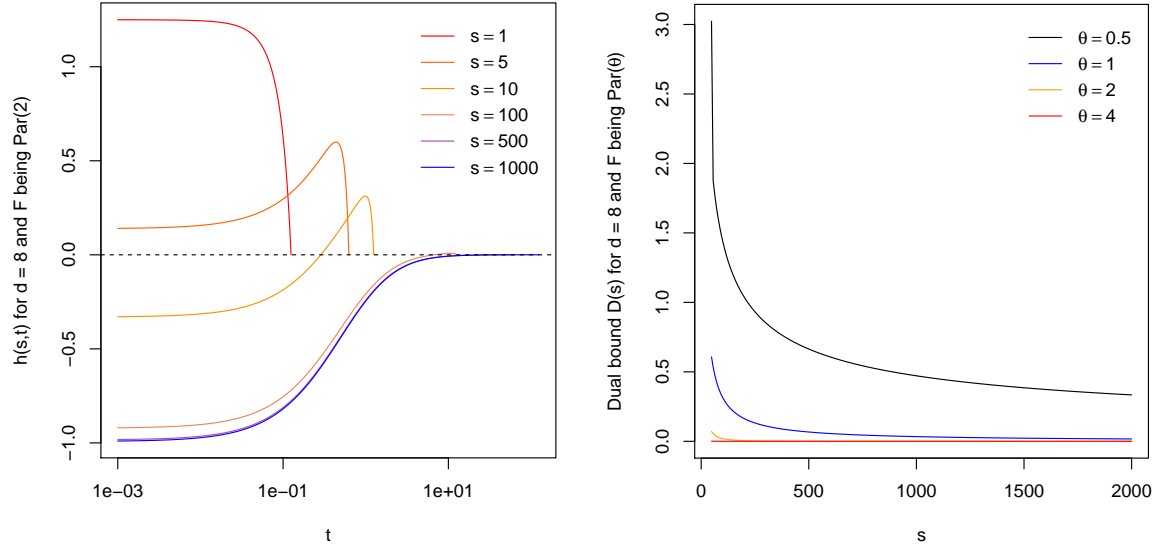


**Figure 1**  $t \mapsto h(s, t)$  for various  $s$ ,  $d = 8$  and  $F$  being Par(2) (left-hand side). The dual bound  $D(s)$  for  $d = 8$  and  $F$  being Par( $\theta$ ) for various parameters  $\theta$  (right-hand side).

### 2.3 Wang's approach for computing $\overline{\text{VaR}}_\alpha(L^+)$

The approach of Embrechts et al. (2014, Proposition 3.1), termed *Wang's approach* here (dating back to work of Ruodu Wang), is conceptually simpler and numerically more stable than the dual bound approach. For notational simplicity, let us introduce

$$a_c = \alpha + (d - 1)c, \quad b_c = 1 - c, \quad (3)$$

for  $c \in [0, (1 - \alpha)/d]$  (so that  $a_c \in [\alpha, 1 - (1 - \alpha)/d]$  and  $b_c \in [1 - (1 - \alpha)/d, 1]$ ). Assume  $F$  admits a density which is positive and decreasing on  $[\beta, \infty)$  for some  $\beta \leq F^-(\alpha)$ . Then, for

## 2 Known optimal solutions in the homogeneous case and their computation

$L \sim F$ ,

$$\overline{\text{VaR}}_\alpha(L^+) = d \mathbb{E}[L \mid L \in [F^-(a_c), F^-(b_c)]], \quad \alpha \in [F(\beta), 1), \quad (4)$$

where  $c$  is the smallest number in  $(0, (1 - \alpha)/d]$ <sup>6</sup> such that

$$\bar{I}(c) := \frac{1}{b_c - a_c} \int_{a_c}^{b_c} F^-(y) dy \geq \frac{d-1}{d} F^-(a_c) + \frac{1}{d} F^-(b_c). \quad (5)$$

Note that  $c$  typically depends on  $d, \alpha$ . Furthermore, in case of  $\text{Par}(\theta)$ ,  $\bar{I}$  is given by

$$\bar{I}(c) = \begin{cases} \frac{1}{b_c - a_c} \frac{\theta}{1-\theta} ((1 - b_c)^{1-1/\theta} - (1 - a_c)^{1-1/\theta}) - 1, & \text{if } \theta \neq 1, \\ \frac{1}{b_c - a_c} \log\left(\frac{1-a_c}{1-b_c}\right) - 1, & \text{if } \theta = 1. \end{cases}$$

The distribution function  $F_{L|L \in [F^-(a_c), F^-(b_c)]}$  of  $L \mid L \in [F^-(a_c), F^-(b_c)]$  is given by  $F_{L|L \in [F^-(a_c), F^-(b_c)]}(x) = \frac{F(x) - a_c}{b_c - a_c}$ ,  $x \in [F^-(a_c), F^-(b_c)]$ . Using this fact and by means of a substitution, we obtain that, for  $\alpha \in [F(\beta), 1)$ , (4) equals

$$\overline{\text{VaR}}_\alpha(L^+) = d \int_{F^-(a_c)}^{F^-(b_c)} x dF_{L|L \in [F^-(a_c), F^-(b_c)]}(x) = d \frac{\int_{F^-(a_c)}^{F^-(b_c)} x dF(x)}{b_c - a_c} = d \bar{I}(c). \quad (6)$$

Equation (6) has the advantage of having the integration in  $\bar{I}(c)$  over a compact interval. Furthermore, finding the smallest  $c$  such that (5) holds also involves  $\bar{I}(c)$ . A procedure thus only needs to know the quantile function  $F^-$  to compute  $\overline{\text{VaR}}_\alpha(L^+)$ . This leads to the following algorithm.

**Algorithm 2.5 (Computing  $\overline{\text{VaR}}_\alpha(L^+)$  according to Wang's approach)**

- 1) Specify an initial interval  $[c_l, c_u]$  with  $c_l \geq 0$  and  $c_u = (1 - \alpha)/d$ .
- 2) Root-finding in  $c$ : Iterate over  $c \in [c_l, c_u]$  until a  $c^*$  is found for which  $h(c^*) = 0$ , where

$$h(c) := \bar{I}(c) - \left( \frac{d-1}{d} F^-(a_c) + \frac{1}{d} F^-(b_c) \right). \quad (7)$$

Then return  $(d-1)F^-(a_{c^*}) + F^-(b_{c^*})$ .

This procedure is implemented in the function `worst_VaR_hom(..., method="Wang")` and `worst_VaR_hom(..., method="Wang.Par")` in the R package `qrmtools`; the latter explicitly implements  $\bar{I}(c)$  for the  $\text{Par}(\theta)$  case.

Let us now address selected properties of the root-finding procedure in Algorithm 2.5.  $\bar{I}$  satisfies  $\bar{I}(0) = \frac{1}{1-\alpha} \int_\alpha^1 F^-(y) dy = \text{ES}_\alpha(L)$ , i.e.,  $\bar{I}(0)$  is the *expected shortfall* of  $L \sim F$  at confidence level  $\alpha$ . If  $L$  has a finite first moment, then  $\bar{I}(0)$  is finite. Therefore,  $h(0)$

<sup>6</sup>In contrast to what is given in Embrechts et al. (2014), this interval has to exclude 0 since otherwise, for  $\text{Par}(\theta)$  margins with  $\theta \in (0, 1]$ ,  $c$  equals 0 and thus, erroneously,  $\overline{\text{VaR}}_\alpha(L^+) = d\bar{I}(0) = \infty$ .

## 2 Known optimal solutions in the homogeneous case and their computation

is finite (if  $F^-(1) < \infty$ ) or  $-\infty$  (if  $F^-(1) = \infty$ ). Either way, we can take  $c_l = 0$  in Step 1) of Algorithm 2.5. However, if  $L \sim F$  has an infinite first moment, then  $\bar{I}(0) = \infty$  and  $F^-(1) = \infty$ , so  $h(0)$  is not defined; this happens, e.g., if  $F$  is  $\text{Par}(\theta)$  with  $\theta \in (0, 1]$ . In this case, we are forced to choose  $c_l \in (0, (1 - \alpha)/d)$ . It remains unclear how this can be done automatically while still guaranteeing that  $h$  has a root on  $[c_l, (1 - \alpha)/d]$ ; `worst_VaR_hom(..., method="Wang.Par")` uses  $c_l = \text{.Machine}\$double.eps$  as a default in this case. Concerning  $c_u$ , note that for  $c_u = (1 - \alpha)/d$ , l'Hospital's Rule implies that  $\bar{I}(c_u) = F^-(\frac{d-1+\alpha}{d})$  and thus that  $h(c_u) = 0$ . We thus have a similar problem (a root at the upper endpoint of the initial interval) as for computing the dual bound and we treat it as described before.

The following proposition provides properties of the crucial function  $h$  (in (7)) for Wang's approach for computing  $\bar{\text{VaR}}_\alpha(L^+)$  in the homogeneous case.

### Proposition 2.6 (Properties of $h$ )

Let  $d \geq 3$ ,  $F$  be a distribution function with a positive density on  $[\beta, \infty)$  and  $\alpha \in [F(\beta), 1)$ . Then

- 1)  $F^-$  equals  $F^{-1}$  on  $[F(\beta), 1]$  and  $F^{-1}$  is strictly increasing and continuous there. Furthermore,  $h$  given by (7) is continuous;
- 2) if  $F^{-1}$  is continuously differentiable,  $h$  has a negative one-sided derivative at the right endpoint; and
- 3) if the density  $f$  of  $F$  is twice continuously differentiable with all derivatives being non-zero everywhere and such that  $3f'(x)^2f(x) - f''(x) < 0$  for all  $x \in (\beta, \infty)$ , then  $h$  is concave.

*Proof.*

- 1) Since  $F$  has a positive density on  $[\beta, \infty)$ ,  $F$  is strictly increasing and continuous there and thus  $F^- = F^{-1}$ , i.e., the ordinary inverse of  $F$ . Furthermore,  $F^{-1}$  is strictly increasing and continuous. The latter immediately implies continuity of  $h$ .
- 2) Let  $a(c) = a_c$ ,  $b(c) = b_c$  for  $a_c, b_c$  as in (3),  $c_l \geq 0$ ,  $c_u = (1 - \alpha)/d$ ,  $c \in (c_l, c_u)$  and  $G = F^{-1}$ , and note that  $a(c_u) = b(c_u) = 1 - (1 - \alpha)/d =: p \in [1 - (1 - F(\beta))/d, 1) \subseteq (F(\beta), 1)$ . The use of a change of variables  $y = r(c, x) := a(c) + (b(c) - a(c))x$  leads to

$$\bar{I}(c) = \frac{\int_{a(c)}^{b(c)} G(y) dy}{b(c) - a(c)} = \int_0^1 G(a(c) + (b(c) - a(c))x) dx = \int_0^1 G(r(c, x)) dx$$

and thus  $h(c) = \int_0^1 G(r(c, x)) dx - \frac{d-1}{d}G(a(c)) - \frac{1}{d}G(b(c))$ . It follows from

$$r(c_u, x) = \alpha + (d - 1)c_u + (1 - \alpha - dc_u)x = p \tag{8}$$



## 2 Known optimal solutions in the homogeneous case and their computation

that  $h(c_u) = G(p) - \frac{d-1}{d}G(p) - \frac{1}{d}G(p) = 0$ . Furthermore,  $a'(c) = d - 1$ ,  $b'(c) = -1$  so that, by Leibniz's rule for differentiation under the integral sign,

$$\begin{aligned} h'(c) &= \int_0^1 G'(r(c, x)) \frac{\partial}{\partial c} r(c, x) dx - \frac{d-1}{d} G'(a(c)) a'(c) - \frac{1}{d} G'(b(c)) b'(c) \\ &= \int_0^1 G'(r(c, x)) (d-1-xd) dx - \frac{(d-1)^2}{d} G'(a(c)) + \frac{1}{d} G'(b(c)) \end{aligned} \quad (9)$$

and thus, by Equation (8),

$$\lim_{c \uparrow c_u} h'(c) = \int_0^1 G'(p) (d-1-xd) dx - \frac{(d-1)^2}{d} G'(p) + \frac{1}{d} G'(p) = G'(p) (1-d/2).$$

The claim follows by noting that  $d \geq 3$  and, by Part 1),  $G$  is strictly increasing, so  $G' > 0$  on  $(F(\beta), 1)$  and thus  $G'(p) > 0$ .

- 3) Let  $f(x) = F'(x) > 0$  be decreasing on  $(\beta, \infty)$ . Then  $G'(y) = 1/f(G(y)) > 0$  and  $G''(y) = -f'(G(y))/f(G(y))^3 > 0$ . Now consider

$$G'''(y) = \frac{3f'(G(y))^2 f(G(y)) - f''(G(y))}{f(G(y))^5},$$

which is negative on  $(F(\beta), 1)$  by assumption. Equation (9) implies that

$$h''(c) = \int_0^1 G''(r(c, x)) ((d-1) - xd)^2 dx - \frac{(d-1)^3}{d} G''(a(c)) - \frac{1}{d} G''(b(c)).$$

Since  $G''' < 0$  on  $(F(\beta), 1)$ ,  $G''$  is decreasing there and thus  $r(c, x) \geq a(c)$  implies  $G''(r(c, x)) \leq G''(a(c))$  for  $x \in [0, 1]$ . It follows that

$$\begin{aligned} h''(c) &\leq G''(a(c)) \int_0^1 ((d-1) - xd)^2 dx - \frac{(d-1)^3}{d} G''(a(c)) - \frac{1}{d} G''(b(c)) \\ &= G''(a(c)) \left( \frac{d^2}{3} - d + 1 \right) - \frac{(d-1)^3}{d} G''(a(c)) - \frac{1}{d} G''(b(c)) \\ &= \frac{1}{d} \left( G''(a(c)) \left( -\frac{2}{3}d^3 + 2d^2 - 2d + 1 \right) - G''(b(c)) \right) \end{aligned}$$

which is negative for all  $d \geq 2$  since  $G'' > 0$  on  $(F(\beta), 1)$ , so  $h$  is concave. □

Given the assumptions stated in Proposition 2.6 hold for the particular  $F$  under consideration,  $h$  is known to have a unique root on  $(0, (1-\alpha)/d)$ .

### Lemma 2.7

Let  $F : (0, 1) \rightarrow \mathbb{R}$  be a locally absolutely continuous function, and let  $\lim_{x \uparrow 1} F(x) = \infty$ . Then  $\limsup_{x \uparrow 1} F'(x) = \infty$ .

## 2 Known optimal solutions in the homogeneous case and their computation

*Proof.* Fix  $a \in (0, 1)$ . For almost all  $x$ ,  $H(x) = H(a) + \int_a^x H'(y) dy$ . If  $H'$  is bounded above by  $K$ , then the second term is bounded above by  $H(a) + K(x - a)$ , contradicting thereby the hypothesis that  $H \rightarrow \infty$  as  $x \rightarrow 1$ .  $\square$

The following is a combination of a stated result (Corollary 3.50 and Exercise 3.51) from G. Leoni, "A First Course in Sobolev Spaces", page 97 (American Mathematical Society, 2009).  $AC_{loc}(I)$  denotes the space of all locally absolutely continuous functions  $u : I \rightarrow \mathbb{R}$ .

### Lemma 2.8

Let  $I, J$  be two intervals, let  $f \in AC_{loc}(J)$  and let  $u : I \rightarrow J$  be monotone and  $AC_{loc}$ . Then  $f \circ u \in AC_{loc}(I)$  and  $(f \circ u)'(x) = f'(u(x))u'(x)$  almost everywhere.

### Lemma 2.9

Let  $H : (0, 1) \rightarrow \mathbb{R}$  be increasing and absolutely continuous. If  $\lim_{x \uparrow 1} H(x) = \infty$  then  $\limsup_{x \uparrow 1} \frac{H'(x)}{H(x)} = \infty$

*Proof.* Let  $F(x) = \log(H(x))$ . By Lemma 2.8,  $F$  is locally absolutely continuous, and  $F' = \frac{H'(x)}{H(x)}$  almost everywhere. The result then follows by Lemma 2.7.  $\square$

### Lemma 2.10

Let  $f$  and  $g$  be functions such that  $\lim_{x \uparrow 1} f(x) = \infty$  and  $\limsup_{x \uparrow 1} \frac{g(x)}{f(x)} = \infty$ , and let  $C_1 > 0, C_2 > 0$ . Then  $\limsup_{x \uparrow 1} C_1 g(x) - C_2 f(x) = \infty$ .

*Proof.* Let  $M > 0$ , and let  $x_n \uparrow 1$  be such that  $\lim_{n \rightarrow \infty} \frac{g(x_n)}{f(x_n)} = \infty$ . There exists  $N_1, N_2$  such that for  $n \geq N_1$ ,  $f(x_n) \geq 1$ , for  $n \geq N_2$ ,  $\frac{g(x_n)}{f(x_n)} \geq \frac{M+C_2}{C_1}$ . Then  $C_1 g(x_n) - C_2 f(x_n) = f(x_n) \left( C_1 \frac{g(x_n)}{f(x_n)} - C_2 \right) \geq M$  for  $n \geq N_0 = \max(N_1, N_2)$ .  $\square$

### Proposition 2.11

Under the assumptions in Proposition 2.6  $h(c)$  has a root in  $(0, 1)$ . Under the additional assumptions making  $h$  strictly concave, the root is unique.

*Proof.* Using the Lemma 2.7 we can see that the (one-sided) derivative of  $h$  at one is negative, so existence of a root will follow if we can show that  $\liminf_{c \downarrow 0} h(c) = -\infty$ . Uniqueness will then follow from strict concavity under the additional assumptions.

Using the definition of  $h$ , and the fact that  $b_c - a_c \rightarrow 1 - \alpha$  as  $c \downarrow 0$ , for any  $k < 1 - \alpha$ , and  $c$  small enough

$$\begin{aligned} h(c) &= \left( \frac{1}{b_c - a_c} \int_{\alpha}^{b_c} G(y) dy - \frac{1}{d} G(b_c) \right) - \left( \frac{1}{b_c - a_c} \int_{\alpha}^{a_c} G(y) dy + \frac{d-1}{d} G(a_c) \right) \\ &\leq \left( \frac{1}{k} \int_{\alpha}^{b_c} G(y) dy - \frac{1}{d} G(b_c) \right) - \left( \frac{1}{b_c - a_c} \int_{\alpha}^{a_c} G(y) dy + \frac{d-1}{d} G(a_c) \right) \\ &= T_1(c) - T_2(c) \end{aligned}$$

## 2 Known optimal solutions in the homogeneous case and their computation

Recalling that  $b_c = 1 - c$ , and the smoothness assumptions on  $G$ , the fact that  $\lim_{c \downarrow 0} G(b_c) = \infty$  implies, after applying Lemmas 2.9 and 2.10 that  $\liminf_{c \downarrow 0} T_1(c) = -\infty$ . Continuity of  $G$  implies that  $\lim_{c \downarrow 0} T_2(c) = \frac{d-1}{d} G(\alpha)$ .  $\square$

**Lemma 2.12 (Examples for which  $h$  has a unique root in  $(0, (1 - \alpha)/d)$ )**

- 1) If  $F$  is the distribution function of the  $N(0, 1)$  distribution, we can take  $\beta \in [1.1, \infty)$  and  $h$  has a unique root in  $(0, (1 - \alpha)/d)$  for all  $\alpha \geq F(\beta)$ .
- 2) If  $F$  is the distribution function of the  $\text{Par}(\theta)$  distribution for any  $\theta > 0$ , we can take  $\beta \in [1.51, \infty)$  and  $h$  has a unique root in  $(0, (1 - \alpha)/d)$  for all  $\alpha \geq F(\beta)$ .

*Proof.*

- 1) In the case of a  $N(0, 1)$  distribution,  $f'(x) = -xf(x)$  and  $f''(x) = -f(x) - xf'(x) = -f(x) + x^2f(x) = f(x)(x^2 - 1)$  are non-zero for all  $x > 1$ . Furthermore,  $3f'(x)^2f(x) - f''(x) = f(x)(1 + x^2(3f(x)^2 - 1))$ . Consider  $g(x) = 1 + x^2(3f(x)^2 - 1)$  and note that  $g(1.1) < 0$  and  $g'(x) < 0$  if  $(-x^2 + 1)e^{-x^2} < \sqrt{2\pi}/3$  which is the case for all  $x > 1$ .
- 2) In the case of a  $\text{Par}(\theta)$  distribution,  $\theta > 0$ ,  $f(x) = \theta(1 + x)^{-\theta-1}$  and thus  $f'(x) = -\theta(\theta + 1)(1 + x)^{-\theta-2}$  and  $f''(x) = \theta(\theta + 1)(\theta + 2)(1 + x)^{-\theta-3}$  are non-zero for all  $x > 0$ . Furthermore,  $3f'(x)^2f(x) - f''(x) = (1 + x)^{-\theta-3}((1 + x)^{-2\theta-2}3\theta^3(\theta + 1)^2 - \theta(\theta + 1)(\theta + 2))$  which is negative for all  $x > 0$  such that  $(1 + x)^{-2\theta-2} < \frac{(\theta+1)(\theta+2)}{3\theta^2(\theta+1)^2}$ , or, equivalently, all  $x > (\frac{2\theta^2(\theta+1)^2}{(\theta+1)(\theta+2)})^{1/(2\theta+2)} - 1 =: g(\theta)$ . Now  $g(\theta) \leq (3(\theta + 1)^2)^{1/(2\theta+2)} - 1 \leq \sqrt{3}(\theta + 1)^{1/(\theta+1)} - 1$ . Note that  $(\theta + 1)^{1/(\theta+1)}$  attains its maximum at  $\theta = e - 1$  and thus  $g(\theta) \leq \sqrt{3}e^{1/e} - 1 \approx 1.502238$ . Therefore, if we choose  $\beta \geq 1.51$ , then the claim holds for all  $\theta > 0$ .  $\square$

**Example 2.13 (Auxiliary function and  $\overline{\text{VaR}}_\alpha(L^+)$  for Wang's approach)**

As an example, consider  $d = 8$   $\text{Par}(\theta)$  risks and confidence level  $\alpha = 0.99$ . Figure 2 illustrates the objective function  $h(c)$  (see (7)) for  $\theta = 2$  (on the left-hand side it is evaluated by numerical integration) and  $\theta = 1/2$  (on the right-hand side it is evaluated analytically) as a function of  $c \in (0, (1 - \alpha)/d]$ . We see that this objective function is flat for small  $\theta$  and this becomes even much flatter for large  $d$ . Finding the root in  $(0, (1 - \alpha)/d)$  is thus challenging from a numerical point of view for small  $\theta$ . This can also be seen from Figure 3 which displays  $\overline{\text{VaR}}_\alpha(L^+)$  as a function in  $1 - \alpha$  for various  $\theta$  and  $d = 8$  (left-hand side) and  $d = 100$  (right-hand side);  $c_l$  was chosen as `.Machine$double.eps` for  $\theta \in \{0.5, 1\}$  as described above. The fact that the objective function  $h$  is flat for small  $\theta$  causes  $\overline{\text{VaR}}_\alpha(L^+)$  to be no longer monotonic in  $\alpha$  and we clearly see how much this affects the computed  $\overline{\text{VaR}}_\alpha(L^+)$ . Possible solutions may involve (much slower) multiple-precision floating-point computations or a smart rescaling of the whole objective function depending on  $\theta$  and  $d$ .

## 2 Known optimal solutions in the homogeneous case and their computation

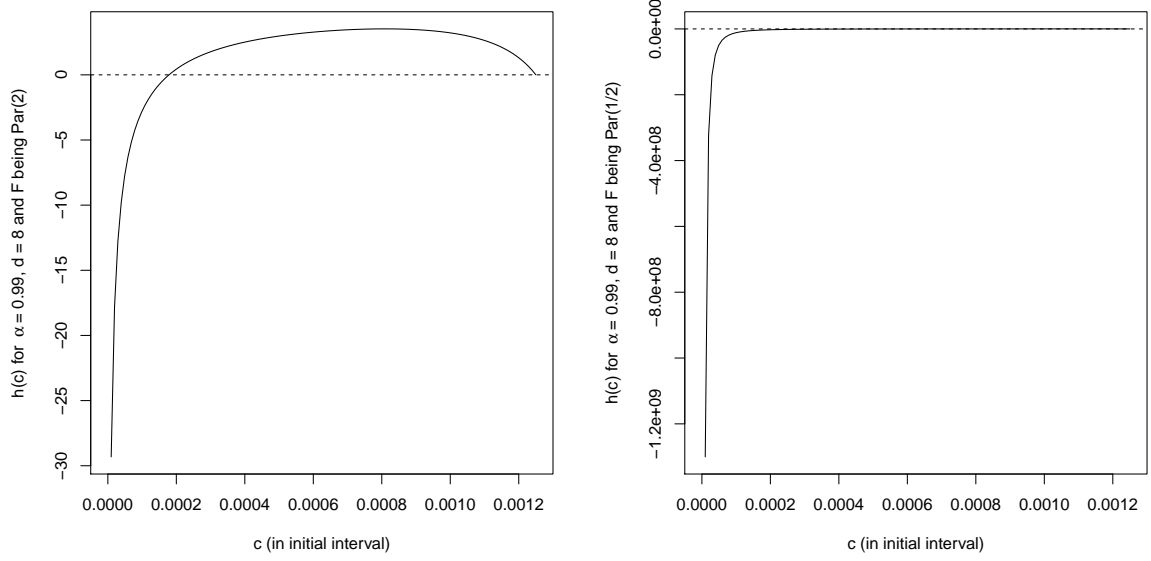


**Figure 2** Objective function  $h(c)$  for  $\alpha = 0.99$ ,  $d = 8$  and  $F$  being  $\text{Par}(2)$  (left-hand side) and  $\text{Par}(1/2)$  (right-hand side).

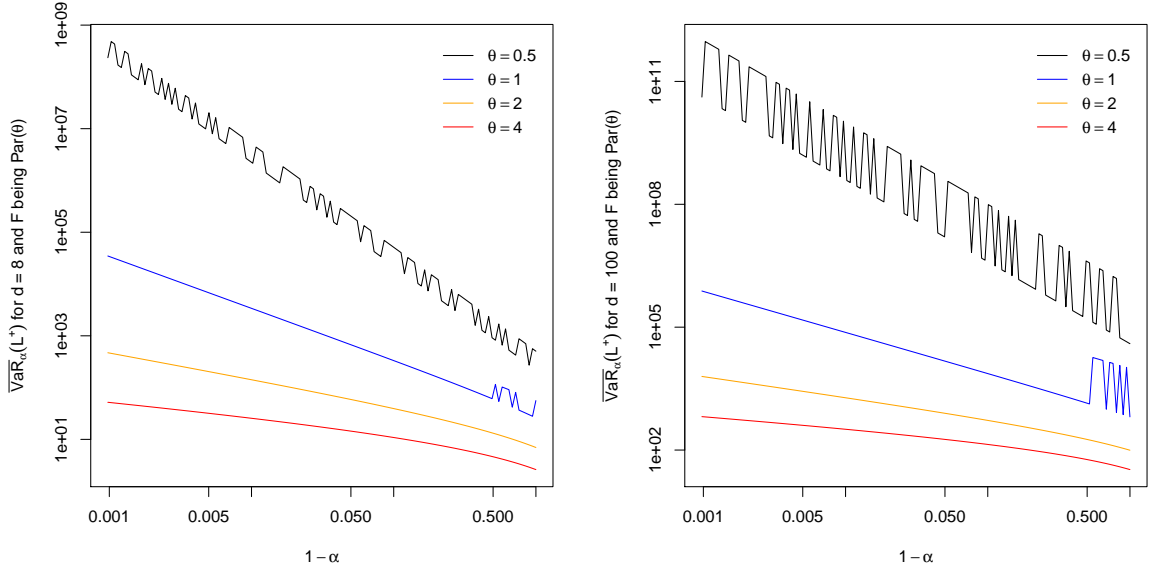


**Figure 3**  $\overline{\text{VaR}}_\alpha(L^+)$  as a function of  $1 - \alpha$  for  $d = 8$  (left-hand side) and  $d = 100$  (right-hand side) and  $F$  being  $\text{Par}(\theta)$  for various parameters  $\theta$ .

### 3 The Rearrangement Algorithm

#### Example 2.14 (Comparison of the approaches)

Again let us consider  $d = 8$   $\text{Par}(\theta)$  risks and confidence level  $\alpha = 0.99$ . We compare Wang's approach (using a numerical integration), Wang's approach (using an analytical formula for the integral  $\bar{I}(c)$ ), the dual bound approach, the lower bound obtained from the RA (with  $\varepsilon = 0.001$ ) (see Section 3) and Wang's approach (with an analytical formula for the integral  $\bar{I}(c)$  and `uniroot()`'s default tolerance). All of the results are divided by the upper bound obtained from the RA to facilitate comparison; see Figure 4. The plot on the left-hand side shows that comparable results are obtained by the different approaches for  $\theta > 1$  and it is important to use a higher default tolerance for `uniroot()` in Wang's approach; this can also be seen from the x axis scale on the left-hand side of Figure 3. The plot on the right-hand side shows that the results vary quite a bit in comparison with the upper bound obtained from the RA for  $\theta \in (0, 1]$ . Due to the extreme heavy-tailedness of the marginal loss distributions, the actual  $\overline{\text{VaR}}_{0.99}(L^+)$  numbers are huge for small  $\theta$ ; see `demo(worst_VaR)`. Note that although we *theoretically* know  $\overline{\text{VaR}}_{0.99}(L^+)$  in this homogeneous case, from a *computational* point of view it remains unclear which of the presented approaches provides the most reliable  $\overline{\text{VaR}}_{0.99}(L^+)$  numbers for  $\theta \in (0, 1]$ . In these heavy-tailed examples it should thus become clear that one has to be extremely careful when implementing a supposedly "explicit solution" for computing  $\overline{\text{VaR}}_{0.99}(L^+)$ . If possible, it is generally a good idea to implement various approaches and to compare them.

## 3 The Rearrangement Algorithm

### 3.1 About the algorithm

One of the early works on finding bounds for  $\text{VaR}_\alpha(L^+)$  including a proof of their sharpness can be found in Makarov (1982), who solves this problem for  $d = 2$ . Later on, Firpo and Ridder (2010) prove these results using copula theory, introducing dependence structures into the above framework and extend Makarov's results to include an arbitrary increasing continuous aggregation function (but they do not prove the sharpness of the bounds, though). Williamson and Downs (1990) develop new methods for calculating convolutions and dependency bounds for the distributions of functions of random variables; they use lower and upper approximations to the desired distribution, containing the representation error, and provide bounds on the errors.

Denuit et al. (1999) extend the above two-dimensional frameworks and show how to compute bounds on the distribution function of  $L^+ = L_1 + \dots + L_d$  for the  $d \geq 3$  case. In a similar work, Cossette et al. (2002) further develop results about  $(L_1, L_2)$  by assuming additional information about the correlation structure of  $(L_1, L_2)$ . They further extend their results to the general multivariate case and propose bounds for continuous and componentwise monotone functions in  $L_1, \dots, L_d$ , assuming that the only available information on  $L_j$  is its distribution function  $F_j$ ,  $j \in \{1, \dots, d\}$ . By relaxing some of the continuity assumptions with respect to the aggregation function, Embrechts et al. (2003)

### 3 The Rearrangement Algorithm

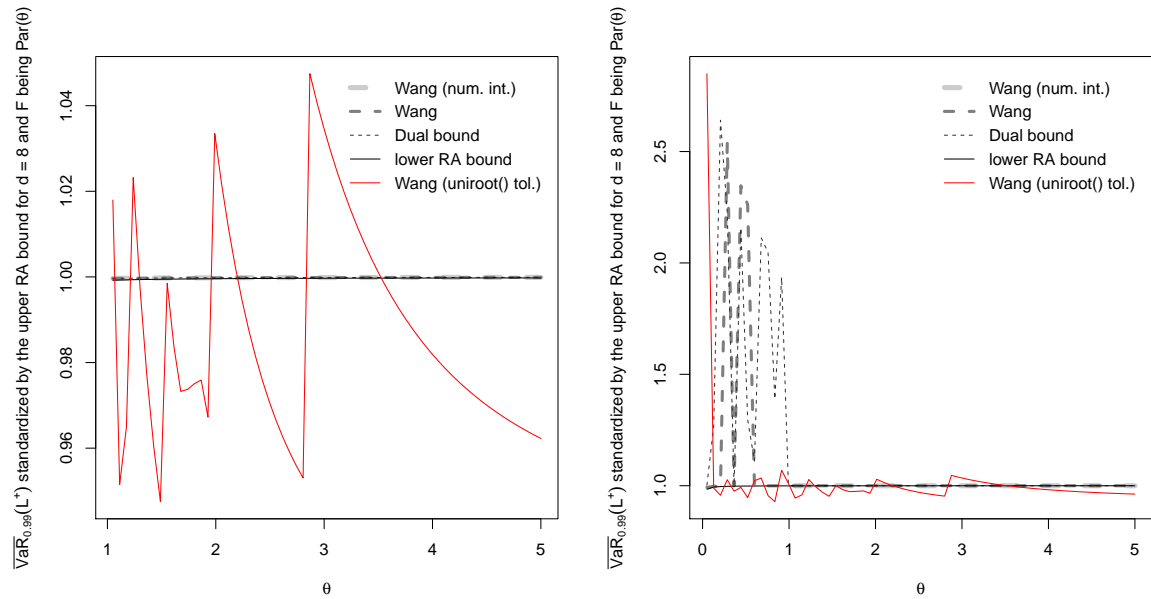


**Figure 4** Comparisons of Wang’s approach (with a numerical integration), Wang’s approach (with an analytical formula for the integral  $\bar{I}(c)$ ), the dual bound approach, the lower bound obtained from the RA and Wang’s approach (with an analytical formula for the integral  $\bar{I}(c)$  and `uniroot()`’s default tolerance). All of the results are divided by the upper bound obtained from the RA to facilitate comparison.

### 3 The Rearrangement Algorithm

provide a generalization of these results using copula theory. In Embrechts et al. (2003) the authors show that without any prior information on the dependence structure, only a *bound* for the distribution function of the sum of the risks can be found and the problem of the *sharpness* of these bounds remained open when  $d \geq 2$ .

Embrechts and Puccetti (2006b) provide better bounds on  $F_{L^+}$  based on the duality result of Rüschendorf (1982) to derive the aforementioned bounds for  $\sum_{j=1}^d L_j$  in the *homogeneous case*  $F_1 = \dots = F_d = F$  for a continuous distribution function  $F$ . This is a rather restrictive assumption especially for large  $d$ . To address this problem, Embrechts and Puccetti (2006a) extend the dual bound approach to general portfolios and describe a numerical procedure to compute these bounds for a non-homogeneous portfolio of risks. The shortcoming of this method is that it requires the application of global optimization algorithms for which there is no guarantee for convergence to a global optimum in a reasonable and predictable amount of time; more importantly the quality of performance of many of these optimization procedures is not well understood and in general the performance of such algorithms deteriorates as  $d$  increases. For these reasons the application of this method for  $d \geq 50$  becomes intractable in some cases.

From the point of view of computational complexity, the above problems can be studied in the context of *completely mixable matrices*, i.e., matrices such that there exists a collection of permutations of columns which result in a constant row sum. If a matrix is not completely mixable, determining the smallest maximal and largest minimal row sums is of interest to find bounds. This problem is in turn connected to discrete approximations (from below for  $\text{VaR}_\alpha(L^+)$  and from above for  $\overline{\text{VaR}}_\alpha(L^+)$ ) of the marginal quantile functions. Haus (2014) points out that such approaches for computing  $\text{VaR}_\alpha$  bounds are related to the multidimensional bottleneck assignment problem and complete mixability is in general  $\mathcal{NP}$ -complete. As a result, convergence to an optimal solution in polynomial time is not guaranteed. If we discretize the tail of each of the  $d$  risk factors using  $N$  points, the underlying space over which the above problems are analyzed becomes an  $N \times d$  matrix and enumeration of the total number of possible matrices arising from permuting all but one column becomes intractable in applications as there are  $(N!)^{d-1}$  possible matrices. One can easily observe that for a portfolio of only 10 positions and  $N = 20$ , the total number of such matrices is  $(20!)^9 \in \mathcal{O}(10^{165})$ . Note that the choices of both  $N = 20$  and  $d = 10$  are extremely conservative and for illustrative purposes only; in practice  $N$  can easily be as large as 1000 to 100 000 and many portfolios consist of at least 20 to 40 instruments; larger financial institutions can have portfolios with several thousand instruments.

As noted earlier, the complexity of the optimization procedures required for finding dual bounds, given arbitrary marginal distributions along with a high run time were the main drawbacks of using the dual bounds approach for obtaining a lower and upper bound for  $\text{VaR}_\alpha(L^+)$ . As a result, Puccetti and Rüschendorf (2012) propose the Rearrangement Algorithm (RA) to tackle these issues. The initial idea underlying the RA and the numerical approximation introduced in Puccetti and Rüschendorf (2012) for calculating  $\text{VaR}_\alpha(L^+)$  and  $\overline{\text{VaR}}_\alpha(L^+)$  is due to Rüschendorf (1983a) and Rüschendorf (1983b), respectively. The higher

### 3 The Rearrangement Algorithm

accuracy of the RA (theoretically still an open question) along with its simple implementation compared to the previous methods makes the RA an attractive alternative for obtaining  $\text{VaR}_\alpha(L^+)$  and  $\overline{\text{VaR}}_\alpha(L^+)$  when (only) the marginal loss distributions  $F_1, \dots, F_d$  are known. In the following section we look at how the RA works and analyze its performance using various test cases.

#### 3.2 How the Rearrangement Algorithm works

The RA can be applied to approximate the best Value-at-Risk  $\text{VaR}_\alpha(L^+)$  or the worst Value-at-Risk  $\overline{\text{VaR}}_\alpha(L^+)$  for any set of marginals  $F_j$ ,  $j \in \{1, \dots, d\}$ . In what follows our focus is on  $\overline{\text{VaR}}_\alpha(L^+)$ . To understand the algorithm, note that two columns  $\mathbf{a}, \mathbf{b} \in \mathbb{R}^N$  are called *oppositely ordered* if for all  $i, j \in \{1, \dots, N\}$  we have  $(a_i - a_j)(b_i - b_j) \leq 0$ . Given a number  $N$  of discretization points of the marginal quantile functions  $F_j^-$ ,  $j \in \{1, \dots, d\}$ , the RA constructs two  $(N, d)$ -matrices, denoted by  $\underline{X}^\alpha$  and  $\overline{X}^\alpha$ ; the first matrix serves to construct an approximation of  $\overline{\text{VaR}}_\alpha(L^+)$  from below, the second matrix is used to construct an approximation of  $\overline{\text{VaR}}_\alpha(L^+)$  from above. Separately for each of these matrices, the RA iterates over its columns and permutes each of them so that it is oppositely ordered to the sum of all other columns. This iteration is repeated until the minimal row sum changes by less than a given  $\varepsilon > 0$ . As Embrechts et al. (2013) state, one then typically ends up with matrices whose minimal row sums are close to each other and roughly equal to  $\overline{\text{VaR}}_\alpha(L^+)$ . Note that if one such iteration over all columns of one of the matrices does not lead to any change in that matrix, then each column of the matrix is oppositely ordered to the sum of all others and thus there is also no change in the minimal row sum.

We provide an adapted version of the RA of Embrechts et al. (2013) for computing  $\overline{\text{VaR}}_\alpha(L^+)$  below. To this end, let

$$s(X) = \min_{1 \leq i \leq N} \sum_{1 \leq j \leq d} x_{ij}$$

denote the minimum of the row sums of an  $(N, d)$ -matrix  $X = (x_{ij})$ . The version of the RA given below contains more information than in Embrechts et al. (2013); e.g., how infinite quantiles are dealt with. For more features of the actual implementation we provide, see the function `RA()` in the R package `qrmtools`. This includes, e.g., a parameter `maxiter` determining the maximal number of iterations or the choice  $\varepsilon = (\text{abs.err}) = \text{NULL}$  (the default) which iterates until each column is oppositely ordered to the sum of all others; note that the latter is typically (by far) not implied by  $\varepsilon = 0$ .

#### Algorithm 3.1 (RA for computing $\overline{\text{VaR}}_\alpha(L^+)$ )

- 1) Fix a confidence level  $\alpha \in (0, 1)$ , marginal quantile functions  $F_1^-, \dots, F_d^-$ , an integer  $N \in \mathbb{N}$  and the desired (absolute) error  $\varepsilon \geq 0$ .
- 2) Compute the lower bound:



### 3 The Rearrangement Algorithm

- 2.1) Define the matrix  $\underline{X}^\alpha = (\underline{x}_{ij}^\alpha)$  for  $\underline{x}_{ij}^\alpha = F_j^-(\alpha + \frac{(1-\alpha)(i-1)}{N})$ ,  $i \in \{1, \dots, N\}$ ,  $j \in \{1, \dots, d\}$ .
- 2.2) Permute randomly the elements in each column of  $\underline{X}^\alpha$ .
- 2.3) For  $1 \leq j \leq d$ , permute the  $j$ -th column of the matrix  $\underline{X}^\alpha$  so that it becomes oppositely ordered to the sum of all other columns. Call the resulting matrix  $\underline{Y}^\alpha$ .
- 2.4) Repeat Step 2.3) until

$$s(\underline{Y}^\alpha) - s(\underline{X}^\alpha) \leq \varepsilon,$$

then set  $\underline{X}^* = \underline{Y}^\alpha$  and  $\underline{s}_N = s(\underline{X}^*)$ .

- 3) Compute the upper bound:

- 3.1) Define the matrix  $\overline{X}^\alpha = (\overline{x}_{ij}^\alpha)$  for  $\overline{x}_{ij}^\alpha = F_j^-(\alpha + \frac{(1-\alpha)i}{N})$ ,  $i \in \{1, \dots, N\}$ ,  $j \in \{1, \dots, d\}$ . If (for  $i = N$  and) for any  $j \in \{1, \dots, d\}$ ,  $F_j^-(1) = \infty$ , adjust it to  $F_j^-(\alpha + \frac{(1-\alpha)(N-1/2)}{N})$ .
- 3.2) Permute randomly the elements in each column of  $\overline{X}^\alpha$ .
- 3.3) For  $1 \leq j \leq d$ , iteratively rearrange the  $j$ -th column of the matrix  $\overline{X}^\alpha$  so that it becomes oppositely ordered to the sum of all other columns. Call the resulting matrix  $\overline{Y}^\alpha$ .
- 3.4) Repeat Step 3.3) until

$$s(\overline{Y}^\alpha) - s(\overline{X}^\alpha) \leq \varepsilon,$$

then set  $\overline{X}^* = \overline{Y}^\alpha$  and  $\overline{s}_N = s(\overline{X}^*)$ .

- 4) Return  $(\underline{s}_N, \overline{s}_N)$ .

The main feature of the RA is the concept of *oppositely ordering* two vectors (step 2.3) against each other, which is designed to reduce the variance of the row sums after each iteration. The randomization of the initial input in (step 2.2) has been put in place to ensure different starting points for each simulation when we calculate  $\overline{\text{VaR}}_\alpha(L^+)$ . Moreover it has been shown that there are certain initial points for which the RA does not converge (see Embrechts et al. (2013) for more details). Randomization of the input matrix aims at reducing the possibility of this happening in practice.

Some words of warning are in order here. Besides the confidence level  $\alpha$  and the marginal quantile functions  $F_1^-, \dots, F_d^-$ , RA relies on two sources of input, namely  $N \in \mathbb{N}$  and  $\varepsilon \geq 0$ , for which Embrechts et al. (2013) do not provide guidance on reasonable defaults, leaving room for interpretation on how to use it. Concerning  $N$ , it obviously needs to be “sufficiently large”, but a practitioner is left alone with such a choice. Another issue is the use of *absolute* error  $\varepsilon$  in the algorithm. There are two problems. The first problem is that

### 3 The Rearrangement Algorithm

it is more natural to use a relative error than an absolute error in this context. Without (roughly) knowing the minimal row sum in Steps 2.4) and 3.4), a pre-specified absolute error does not guarantee that the change in the minimal row sum from  $\underline{X}^\alpha$  to  $\underline{Y}^\alpha$  is of the right order (and such order depends at least on  $d$  and the chosen quantile functions). If  $\varepsilon$  is chosen to be too large, the computed bounds  $\underline{s}_N$  and  $\bar{s}_N$  would carry too much uncertainty, whereas if it is too small, the RA has an unnecessarily long run time; the latter seems to be the case for Embrechts et al. (2013, Table 3), where the chosen  $\varepsilon = 0.1$  is roughly 0.000004% of the computed  $\overline{\text{VaR}}_\alpha(L^+)$  (for  $\alpha = 0.99$ ), with a small absolute error. The second problem is that the absolute error  $\varepsilon$  is only used *individually* for checking “convergence” of  $\underline{s}_N$  and of  $\bar{s}_N$ . It does not guarantee that  $\underline{s}_N$  and  $\bar{s}_N$  are sufficiently close to obtain a reasonable approximation to  $\overline{\text{VaR}}_\alpha(L^+)$ . We are aware of the theoretical hurdles underlying the algorithm which are still open questions at this point (e.g., the probability of convergence of  $\underline{s}_N$  and  $\bar{s}_N$  to  $\overline{\text{VaR}}_\alpha(L^+)$  or that  $\overline{\text{VaR}}_\alpha(L^+) \leq \bar{s}_N$  for sufficiently large  $N$ ), but from a computational point of view one should still check that  $\underline{s}_N$  and  $\bar{s}_N$  are close to each other. Also, the algorithm should return convergence and other useful information, e.g., the relative dependence uncertainty spread (i.e., the relative error  $|(\bar{s}_N - \underline{s}_N)/\bar{s}_N|$ ), the actual absolute errors reached for each of the bounds, the number of iterations used, the actual minimal row sums computed after each iteration or the actual number of oppositely ordered columns determined from the final matrices; see `RA()` in the R package `qrmtools` for such information.

### 3.3 Empirical performance under various setups

In order to empirically investigate the performance of the RA, we consider 8 scenarios. Each scenario consists of one out of two studies and one out of four cases, described in what follows.

As studies, we consider the following:

Study 1.  $N \in \{2^7, 2^8, \dots, 2^{17}\}$  and  $d = 20$ .

Study 2.  $N = 2^8 = 256$  and  $d \in \{2^2, 2^3, \dots, 2^{10}\}$ .

These choices allow us to investigate the impact of the upper tail discretization parameter  $N$  (Study 1.) and the impact of the number of risk factors  $d$  (within a reasonable span; (Study 2.)) on the performance of the RA. The case of  $d = 2$  is included for pedagogical reasons, sorting each column and oppositely ordering them results in an instant optimal solution.

The different cases we consider specify different marginal tail behaviors based on the Pareto distribution with the following distribution function

$$F_j(x) = 1 - (1 + x)^{-\theta_j}, \quad x \geq 0,$$

for a given tail parameter  $\theta_j > 0$ .

### 3 The Rearrangement Algorithm

- Case 1.  $\theta_1, \dots, \theta_d$  are uniformly chosen from 0.6 to 0.4; this case represents a portfolio with a similar marginal tail behavior (a heavy-tailed distribution).
- Case 2.  $\theta_1, \dots, \theta_d$  are uniformly chosen from 0.5 to 1.5; this case represents a portfolio with a different marginal tail behavior (from a very heavy-tailed distribution to a not so heavy-tailed distribution).
- Case 3.  $\theta_1, \dots, \theta_d$  are uniformly chosen from 1.4 to 1.6; this case represents a portfolio with similar marginal tail behavior (a not so heavy-tailed distribution).
- Case 4.  $\theta_2, \dots, \theta_d$  are chosen as in Case 3. and  $\theta_1 = 0.5$ ; this case represents a portfolio with one heavy-tailed marginal loss distribution.

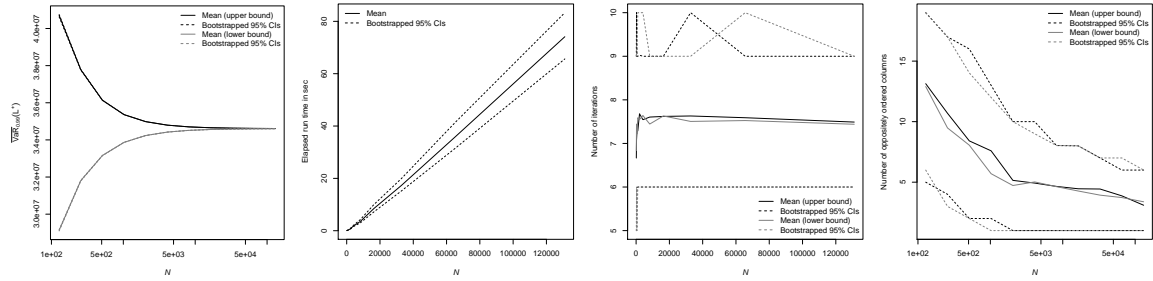


**Figure 5** Study 1, Case 1 (from left to right):  $\text{VaR}_{0.99}$  bounds, run time, number of iterations at convergence and number of oppositely ordered columns.

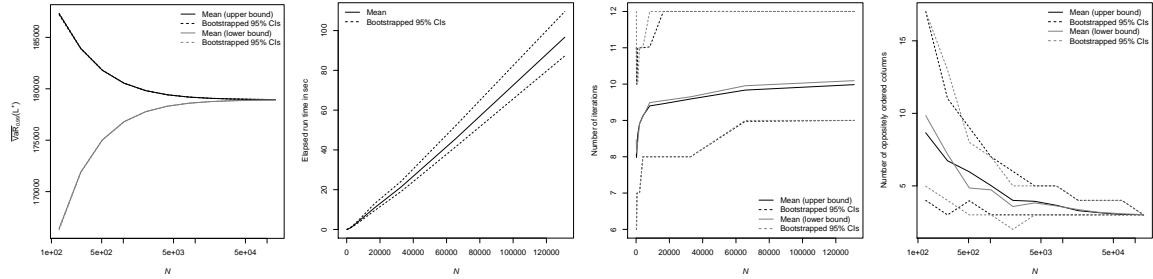


**Figure 6** Study 1, Case 2 (from left to right):  $\text{VaR}_{0.99}$  bounds, run time, number of iterations at convergence and number of oppositely ordered columns.

### 3 The Rearrangement Algorithm

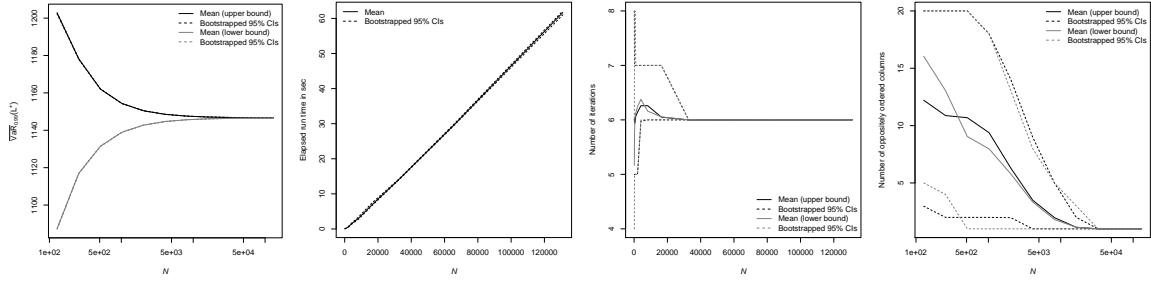


**Figure 7** Study 1, Case 3 (from left to right):  $\text{VaR}_{0.99}$  bounds, run time, number of iterations at convergence and number of oppositely ordered columns.

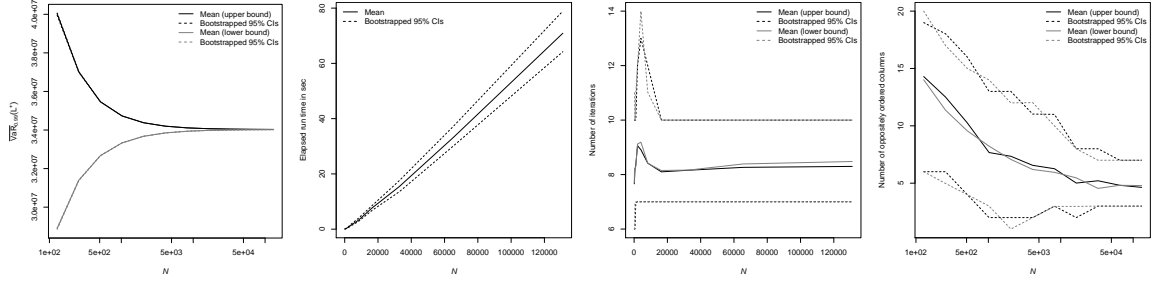


**Figure 8** Study 1, Case 4 (from left to right):  $\text{VaR}_{0.99}$  bounds, run time, number of iterations at convergence and number of oppositely ordered columns.

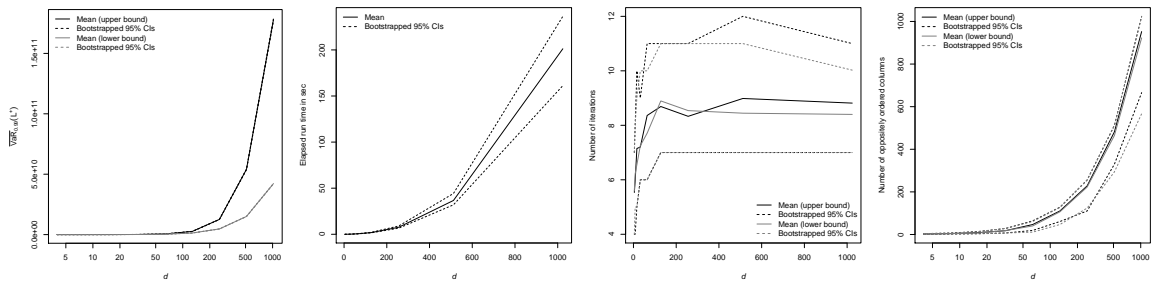


**Figure 9** Study 2, Case 1 (from left to right):  $\text{VaR}_{0.99}$  bounds, run time, number of iterations at convergence and number of oppositely ordered columns.

### 3 The Rearrangement Algorithm

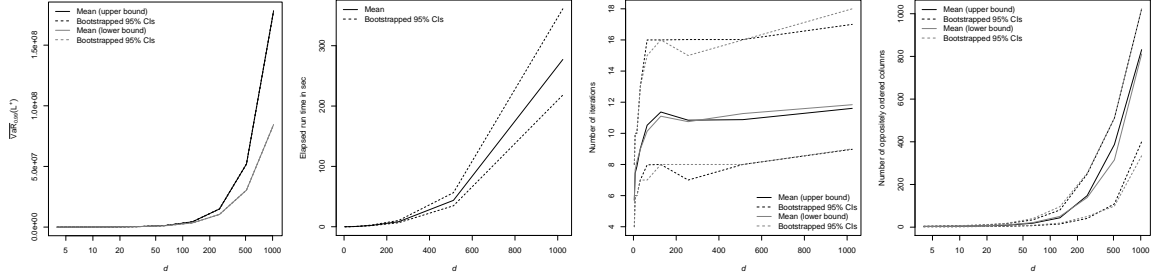


**Figure 10** Study 2, Case 2 (from left to right):  $\text{VaR}_{0.99}$  bounds, run time, number of iterations at convergence and number of oppositely ordered columns.

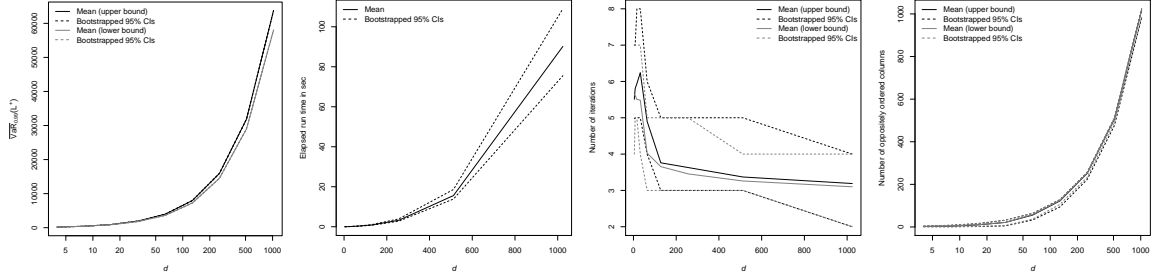


**Figure 11** Study 2, Case 3 (from left to right):  $\text{VaR}_{0.99}$  bounds, run time, number of iterations at convergence and number of oppositely ordered columns.

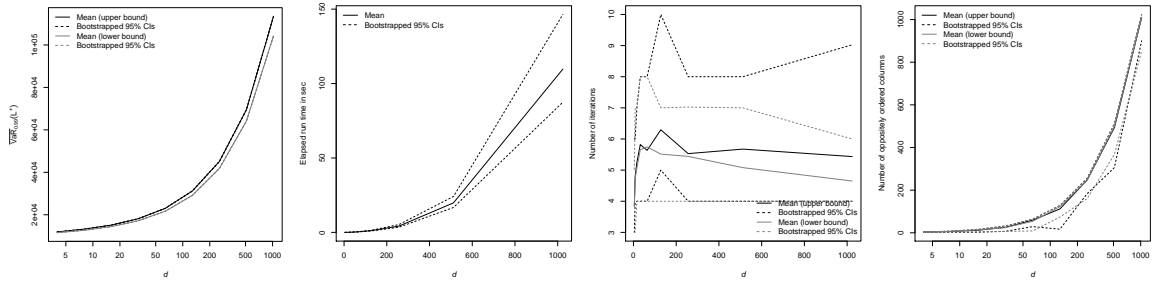


**Figure 12** Study 2, Case 4 (from left to right):  $\text{VaR}_{0.99}$  bounds, run time, number of iterations at convergence and number of oppositely ordered columns.

### 3 The Rearrangement Algorithm

The results presented for each scenario are based on  $B = 200$  simulations run on an AMD 3.2 GHz Phenom II X4 955 processor (with 8 GB RAM). The simulation results for Study 1. can be summarized as follows:

- As it can be seen in the first graphs of figures (5), (6), (7) and (8), both the mean upper bound and mean lower bound of  $\text{VaR}_{0.99}$  converge as  $N$  increases.
- The second graphs in figures (5), (6), (7) and (8) indicate that as  $N$  increases, so does the mean elapsed time; the mean run time in figure (7) is the smallest with the least variability compared to all other cases due to the particular choice of Pareto distribution parameter.
- The third graphs in figures (5), (6), (7) and (8) show that the maximum of number of iterations hardly exceeds 10 as  $N$  increases; this is an important observation as it will be used later on in the choice of the maximum number of iterations required in the ARA.
- Finally, the last graphs indicate that the rate at which the number of oppositely ordered columns decreases depends on the distribution characteristics of the input matrix  $X$ ; The first and last graphs in column 4 follow the same pattern, as the presence of a large first column (due to  $\theta_1 = 0.5$ ) in both cases dominates the variability of the number of oppositely ordered columns.

Figures (9), (10), (11) and (12) show the performance of the RA in the second study; here we are more interested in analyzing the impact of the number of risk factors,  $d$ , on portfolios which exhibit different marginal tail behaviors. Based on 200 simulations of the performance of the RA in each case:

- The first graphs in figures (9), (10), (11) and (12) exhibit the same pattern: the mean upper bound and mean lower bound for  $\text{VaR}_{0.99}$  diverge from one another; this is due to the fact that we have kept  $N$  the same for all cases in Study 2..
- Similar to what we have seen in Study 1., the second graphs in Study 2. indicate that the mean run time of RA increases as the number of risk factors goes up; the third case in Study 2. has the least run time on average as  $\theta_1, \dots, \theta_d$  uniformly chosen in  $[1.4, 1.6]$  will result in smaller elements of the input matrix  $X$  with a smaller range of entries compared to other cases.
- The mean number of iterations at convergence is consistently below 12 across all cases; more important is the uniform behaviour of the mean number of iterations at convergence as  $d$  increases: as can be seen in the third graph, in each case this number remains stable around the mean for large  $d$ 's ( $d \geq 128$ ) and the fact that the upper and lower confidence bounds exhibit the same pattern.
- The number of oppositely ordered columns in each case increases as  $d$  increases; note that this finding does not contradict what we have seen in the first study as we have kept  $N$  the same here.

In the next section we will introduce the *Adaptive Rearrangement Algorithm* and show how

the observations that we have made in this section help us set meaningful initial values of the parameters that are used in the proposed algorithm.

## 4 The Adaptive Rearrangement Algorithm

### 4.1 How the Adaptive Rearrangement Algorithm works

In this section we present an adaptive version of the RA, termed *Adaptive Rearrangement Algorithm (ARA)*. This algorithm for computing bounds for  $\text{VaR}_\alpha(L^+)$  or  $\overline{\text{VaR}}_\alpha(L^+)$  (as before, we focus on the latter) provides an algorithmically improved version of the RA, has more meaningful tuning parameters and adaptively chooses the number of discretization points. The ARA is implemented in the R package `qrmtools`, see the function `ARA()`. Similar to our `RA()` implementation, `ARA()` returns much more information, but the essential part of the algorithm is given as follows.

#### Algorithm 4.1 (ARA for computing $\overline{\text{VaR}}_\alpha(L^+)$ )

- 1) Fix a confidence level  $\alpha \in (0, 1)$ , marginal quantile functions  $F_1^-, \dots, F_d^-$ , an integer vector  $\mathbf{N} \in \mathbb{N}^k$ ,  $k \in \mathbb{N}$ , (containing the numbers of discretization points which are adaptively used), a bivariate vector of relative errors  $\varepsilon = (\varepsilon_1, \varepsilon_2)$  (containing the individual relative error  $\varepsilon_1$  and the joint relative error  $\varepsilon_2$ ; see below) and the maximal number of iterations used for each  $N \in \mathbf{N}$ .

- 2) For  $N \in \mathbf{N}$ , do:

- 2.1) Compute the lower bound:

- 2.1.1) Define the matrix  $\underline{X}^\alpha = (\underline{x}_{ij}^\alpha)$  for  $\underline{x}_{ij}^\alpha = F_j^-(\alpha + \frac{(1-\alpha)(i-1)}{N})$ ,  $i \in \{1, \dots, N\}$ ,  $j \in \{1, \dots, d\}$ .

- 2.1.2) Permute randomly the elements in each column of  $\underline{X}^\alpha$ .

- 2.1.3) For  $j \in \{1, \dots, d\}$ , permute the  $j$ -th column of the matrix  $\underline{X}^\alpha$  so that it becomes oppositely ordered to the sum of all other columns. Call the resulting matrix  $\underline{Y}^\alpha$ .

- 2.1.4) Repeat Step 2.1.3) until

$$\left| \frac{s(\underline{Y}^\alpha) - s(\underline{X}^\alpha)}{s(\underline{X}^\alpha)} \right| \leq \varepsilon_1 \quad (10)$$

or until the specified maximal number of iterations has been reached. Then set  $\underline{X}^* = \underline{Y}^\alpha$  and  $\underline{s}_N = s(\underline{X}^*)$ .

- 2.2) Compute the upper bound:

## 4 The Adaptive Rearrangement Algorithm

- 2.2.1) Define the matrix  $\bar{X}^\alpha = (\bar{x}_{ij}^\alpha)$  for  $\bar{x}_{ij}^\alpha = F_j^-(\alpha + \frac{(1-\alpha)i}{N})$ ,  $i \in \{1, \dots, N\}$ ,  $j \in \{1, \dots, d\}$ . If (for  $i = N$  and) for any  $j \in \{1, \dots, d\}$ ,  $F_j^-(1) = \infty$ , adjust it to  $F_j^-(\alpha + \frac{(1-\alpha)(N-1/2)}{N})$ .
- 2.2.2) Permute randomly the elements in each column of  $\bar{X}^\alpha$ .
- 2.2.3) For  $j \in \{1, \dots, d\}$ , iteratively rearrange the  $j$ -th column of the matrix  $\bar{X}^\alpha$  so that it becomes oppositely ordered to the sum of all other columns. Call the resulting matrix  $\bar{Y}^\alpha$ .
- 2.2.4) Repeat Step 2.2.3) until

$$\left| \frac{s(\bar{Y}^\alpha) - s(\bar{X}^\alpha)}{s(\bar{X}^\alpha)} \right| \leq \varepsilon_1, \quad (11)$$

or until the specified maximal number of iterations has been reached. Then set  $\bar{X}^* = \bar{Y}^\alpha$  and  $\bar{s}_N = s(\bar{X}^*)$ .

- 2.3) Determine convergence based on both the individual and the joint relative errors:

$$\text{If (10) and (11) hold, and if } \left| \frac{\bar{s}_N - \underline{s}_N}{\bar{s}_N} \right| \leq \varepsilon_2 \text{ then break.}$$

- 3) Return  $(\underline{s}_N, \bar{s}_N)$ .

Concerning the choices of tuning parameters in Algorithm 4.1, note that if  $\mathbf{N} = (N)$ , so we have a single number of discretization points, then the ARA reduces to the RA but uses the more meaningful relative instead of absolute errors and not only checks what we termed *individual errors*, i.e., the errors for checking “convergence” of  $\underline{s}_N$  and of  $\bar{s}_N$ , but also the *joint error*, i.e., the relative error between  $\underline{s}_N$  and  $\bar{s}_N$ . As our simulation studies in Section 3.3 suggest, useful (conservative) defaults for  $\mathbf{N}$  and the maximal number of iterations are  $\mathbf{N} = (2^8, 2^9, \dots, 2^{20})$  and 10, respectively. Given the high model uncertainty and the (often) rather large values of  $\text{VaR}_\alpha(L^+)$  (especially in heavy-tailed test cases), a useful (conservative) choice for the relative errors  $\varepsilon$  may be  $\varepsilon = (0.01, 0.01)$  (relative changes/differences of 1%); obviously, all these values can be freely chosen in the actual implementation of `ARA()`.

### 4.2 Empirical performance under various setups

As we explained earlier, one of the main features of the ARA is the *dynamic* choice of the upper tail discretization parameter  $N$ ; therefore in defining the main studies under which the performance of the ARA is analyzed, the choice of  $N$  plays no role; instead we consider two main studies, the first one with  $d = 20$  and the second with  $d = 100$  risk factors.

Under each scenario we investigate 12 examples each of which consists of one the 4 cases with different marginal tail behaviors based on the Pareto distribution, described earlier in



## 4 The Adaptive Rearrangement Algorithm

section 3.3 coupled with one of the following three choices of the bivariate vector of relative errors  $\varepsilon = (\varepsilon_1, \varepsilon_2)$  defined as:

- 1)  $\varepsilon = (0.1\%, 0.5\%)$ , i.e. individual relative error  $\varepsilon_1$  is chosen as 0.1% and the joint relative error  $\varepsilon_2$  is 0.5%.
- 2)  $\varepsilon = (0.1\%, 1\%)$ ; i.e. individual relative error  $\varepsilon_1$  is the same as before and the joint relative error  $\varepsilon_2$  is twice the previous case.
- 3)  $\varepsilon = (0.1\%, 2\%)$ ; individual relative error  $\varepsilon_1$  is kept at the same level and we have doubled the joint relative error  $\varepsilon_2$ .

Therefore the performance of ARA is investigated in 24 different situations. As before, the results shown for each test are based on  $B = 200$  simulations and we report the mean and 95% confidence interval for the lower and upper bounds of  $\text{VaR}_{0.99}$ , the  $N$  used in final iteration of ARA, mean and confidence interval for each example in table (1) as well as the number of oppositely ordered columns and number of iterations for each example in table (2). Our findings indicate that:

- Although in both studies ( $d = 20$  and  $d = 100$ ), the length of the confidence intervals for  $\text{VaR}_{0.99}$  increases as the joint relative error,  $\varepsilon_2$  increases, the mean and lower and upper confidence bounds for  $\text{VaR}_{0.99}$  remain fairly close to each other and within these bounds. More importantly for a fixed level of individual relative error, as  $\varepsilon_2$  increases, we do not observe a drastic shift in both lower and upper bounds for the mean across different examples.
- $N$  used in the final iteration of ARA is shown in the second column; an important observation about this parameter is that in virtually all examples, both the upper and lower bounds for the 95% confidence interval of  $N$  used remain the same; this fact can be leveraged in practice for portfolios which exhibit the same marginal tail behavior to reduce the run time of the ARA.
- The last column in table (1) shows the mean run time of the ARA in each of the 24 examples; it can be seen that doubling the joint relative error reduces the run time more than 50% across all examples.
- The mean number of iterations as well as both the lower and upper bound consistently remain below 5.
- Finally figures 13, 17, 15, 16, and 14 can shed some light on the impact of the randomization of the initial input matrix  $X$ . As it can be seen from our simulations, randomizing the input has a minimal impact on various outputs of the ARA.

## 4 The Adaptive Rearrangement Algorithm

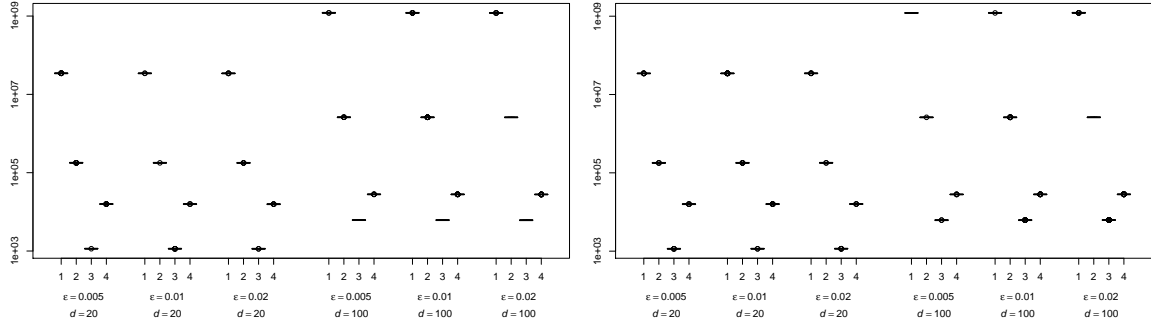


**Figure 13** Boxplots of lower (left-hand side) and upper (right-hand side)  $\overline{\text{VaR}}_{0.99}$  bounds computed with the ARA based on  $B = 200$  replications.

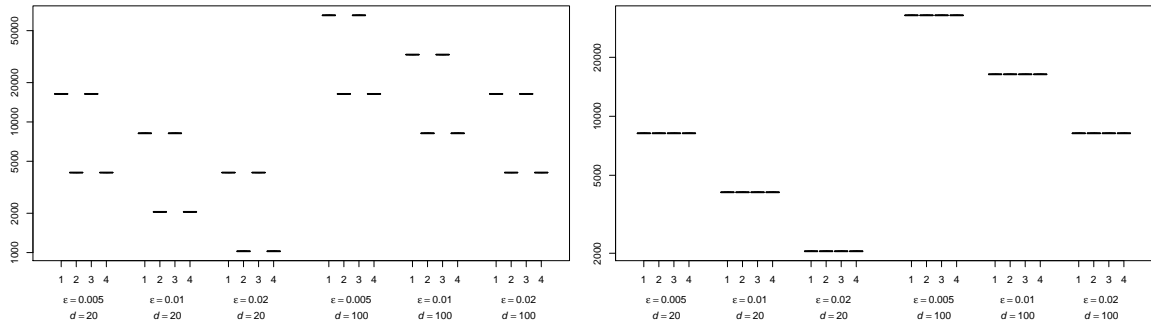


**Figure 14** Boxplots of the actual  $N$  used for computing lower (left-hand side) and upper (right-hand side)  $\overline{\text{VaR}}_{0.99}$  bounds with the ARA based on  $B = 200$  replications.

## 4 The Adaptive Rearrangement Algorithm

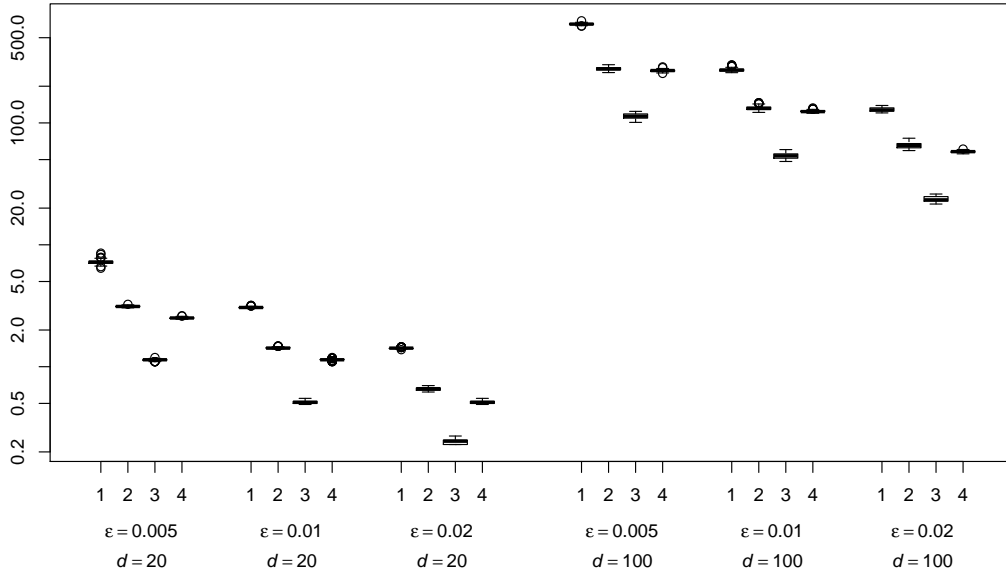


**Figure 15** Boxplots of the run time for computing  $\overline{\text{VaR}}_{0.99}$  bounds with the ARA based on  $B = 200$  replications.

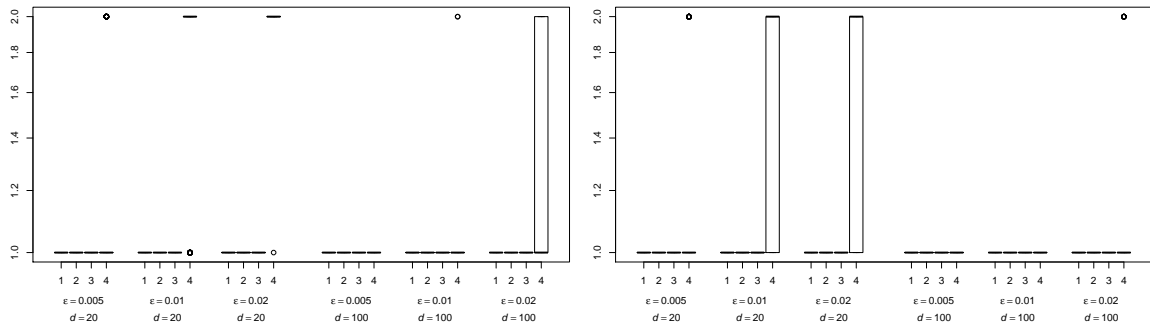


**Figure 16** Boxplots of the number of oppositely ordered columns for computing lower (left-hand side) and upper (right-hand side)  $\overline{\text{VaR}}_{0.99}$  bounds with the ARA based on  $B = 200$  replications.

## 4 The Adaptive Rearrangement Algorithm

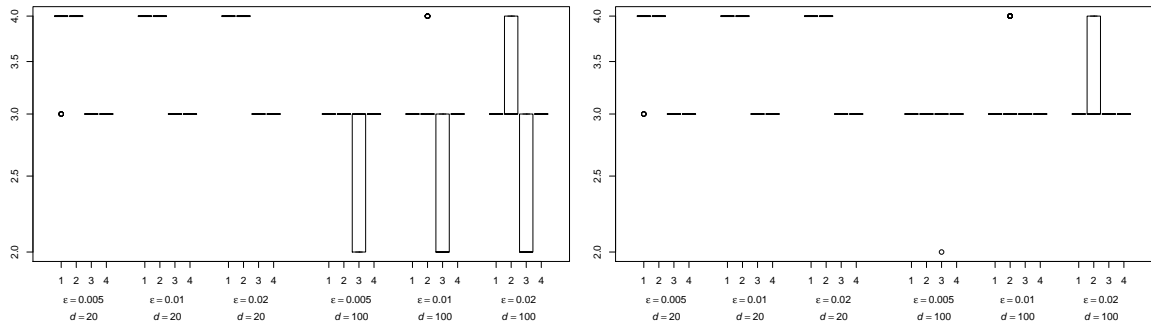


**Figure 17** Boxplots of the number of iterations for computing lower (left-hand side) and upper (right-hand side)  $\overline{\text{VaR}}_{0.99}$  bounds with the ARA based on  $B = 200$  replications.

## 4 The Adaptive Rearrangement Algorithm

$d$	$\varepsilon$ (in %)	Case	$\overline{\text{VaR}}_{0.99}$				$N$ used				Time (in s)	
			Lower		Upper		Lower		Upper		Mean	95% CI
			Mean	95% CI	Mean	95% CI	Mean	95% CI	Mean	95% CI		
20	(0.1, 0.5)	1	3.4592e7	(3.4559e7, 3.4560e7)	3.4653e7	(3.4653e7, 3.4654e7)	16384	(16384, 16384)	8192	(8192, 8192)	7.21	(6.79, 7.76)
		2	1.7857e5	(1.7857e5, 1.7857e5)	1.7916e5	(1.7916e5, 1.7917e5)	4096	(4096, 4096)	8192	(8192, 8192)	3.12	(3.06, 3.20)
		3	1.1446e3	(1.1446e3, 1.1446e3)	1.1484e3	(1.1484e3, 1.1484e3)	16384	(16384, 16384)	8192	(8192, 8192)	1.14	(1.10, 1.17)
		4	1.5839e4	(1.5839e4, 1.5840e4)	1.5905e4	(1.5905e4, 1.5905e4)	4096	(4096, 4096)	8192	(8192, 8192)	2.51	(2.45, 2.57)
	(0.1, 1)	1	3.4513e7	(3.4513e7, 3.4513e7)	3.4700e7	(3.4700e7, 3.4700e7)	8192	(8192, 8192)	4096	(4096, 4096)	3.06	(3.02, 3.13)
		2	1.7827e5	(1.7827e4, 1.7828e4)	1.7938e5	(1.7937e5, 1.7939e5)	2048	(2048, 2048)	4096	(4096, 4096)	1.42	(1.40, 1.46)
		3	1.1426e3	(1.1426e3, 1.1427e3)	1.1530e3	(1.1503e3, 1.1503e3)	8192	(8192, 8192)	4096	(4096, 4096)	0.51	(0.49, 0.54)
		4	1.5807e4	(1.5807e4, 1.5807e4)	1.5938e4	(1.5938e4, 1.5938e4)	2048	(2048, 2048)	4096	(4096, 4096)	1.14	(1.11, 1.17)
	(0.1, 2)	1	3.4420e7	(3.4419e7, 3.4420e7)	3.4793e7	(3.4793e7, 3.4794e7)	4096	(4096, 4096)	2048	(2048, 2048)	1.41	(1.40, 1.45)
		2	1.7773e5	(1.7772e5, 1.7774e5)	1.7978e5	(1.7976e5, 1.7979e5)	1024	(1024, 1024)	2048	(2048, 2048)	0.65	(0.64, 0.69)
		3	1.1389e3	(1.1388e3, 1.1389e3)	1.1542e3	(1.1541e3, 1.1542e3)	4096	(4096, 4096)	2048	(2048, 2048)	0.24	(0.23, 0.26)
		4	1.5739e4	(1.5738e4, 1.5739e4)	1.5991e4	(1.5990e4, 1.5991e4)	1024	(1024, 1024)	2048	(2048, 2048)	0.51	(0.49, 0.55)
100	(0.1, 0.5)	1	1.2054e9	(1.2054e9, 1.2054e9)	1.2095e9	(1.2095e9, 1.2095e9)	65536	(65536, 65536)	32768	(32768, 32768)	647.25	(629.52, 666.05)
		2	2.6073e7	(2.6073e7, 2.6074e7)	2.6162e7	(2.6162e7, 2.6163e7)	16384	(16384, 16384)	32768	(32768, 32768)	278.24	(263.75, 295.46)
		3	6.1760e3	(6.1759e3, 6.1761e3)	6.2018e3	(6.2018e3, 6.2018e3)	65536	(65536, 65536)	32768	(32768, 32768)	113.72	(104.28, 122.44)
		4	2.8035e4	(2.8035e4, 2.8035e4)	2.8156e4	(2.8156e4, 2.8156e4)	16384	(16384, 16384)	32768	(32768, 32768)	268.64	(259.07, 279.24)
	(0.1, 1)	1	1.2034e9	(1.2033e9, 1.2034e9)	1.2116e9	(1.2116e9, 1.2116e9)	32768	(32768, 32768)	16384	(16384, 16384)	271.93	(261.79, 292.40)
		2	2.6029e7	(2.6028e7, 2.6032e7)	2.6194e7	(2.6194e7, 2.6196e7)	8192	(8192, 8192)	16384	(16384, 16384)	132.27	(125.50, 143.53)
		3	6.1631e3	(6.1630e3, 6.1632e3)	6.2148e3	(6.2148e3, 6.2148e3)	32768	(32768, 32768)	16384	(16384, 16384)	53.62	(49.04, 58.60)
		4	2.7972e4	(2.7972e4, 2.7972e4)	2.8212e4	(2.8212e4, 2.8212e4)	8192	(8192, 8192)	16384	(16384, 16384)	124.57	(120.94, 129.17)
	(0.1, 2)	1	1.1992e9	(1.1992e9, 1.1993e9)	1.2157e9	(1.2157e9, 1.2157e9)	16384	(16384, 16384)	8192	(8192, 8192)	128.66	(121.98, 136.47)
		2	2.5950e7	(2.5948e7, 2.5952e7)	2.6252e7	(2.6250e7, 2.6254e7)	4096	(4096, 4096)	8192	(8192, 8192)	65.48	(60.17, 74.24)
		3	6.1379e3	(6.1378e3, 6.1380e3)	6.2412e3	(6.2411e3, 6.2412e3)	16384	(16384, 16384)	8192	(8192, 8192)	23.73	(22.16, 25.74)
		4	2.7853e4	(2.7853e4, 2.7853e4)	2.8278e4	(2.8278e4, 2.8278e4)	4096	(4096, 4096)	8192	(8192, 8192)	58.15	(56.45, 60.14)

**Table 1** Results for computing  $\overline{\text{VaR}}_{0.99}$  with the ARA based on  $B = 200$  bootstrap replications.

## 5 Conclusion

$d$	$\varepsilon$ (in %)	Case	Number of oppositely ordered columns				Number of iterations			
			Lower		Upper		Lower		Upper	
			Mean	95% CI	Mean	95% CI	Mean	95% CI	Mean	95% CI
20	(0.1, 0.5)	1	1	(1,1)	1	(1,1)	3.975	(3.975,4)	3.98	(4,4)
		2	1	(1,1)	1	(1,1)	4	(4,4)	4	(4,4)
		3	1	(1,1)	1	(1,1)	3	(3,3)	3	(3,3)
		4	1.195	(1,2)	1.12	(1,2)	3	(3,3)	3	(3,3)
	(0.1, 1)	1	1	(1,1)	1	(1,1)	4	(4,4)	4	(4,4)
		2	1	(1,1)	1	(1,1)	4	(4,4)	4	(4,4)
		3	1	(1,1)	1	(1,1)	3	(3,3)	3	(3,3)
		4	1.795	(1,2)	1.715	(1,2)	3	(3,3)	3	(3,3)
	(0.1, 2)	1	1	(1,1)	1	(1,1)	4	(4,4)	4	(4,4)
		2	1	(1,1)	1	(1,1)	4	(4,4)	4	(4,4)
		3	1	(1,1)	1	(1,1)	3	(3,3)	3	(3,3)
		4	1.995	(2,2)	1.67	(1,2)	3	(3,3)	3	(3,3)
100	(0.1, 0.5)	1	1	(1,1)	1	(1,1)	3	(3,3)	3	(3,3)
		2	1	(1,1)	1	(1,1)	3	(3,3)	3	(3,3)
		3	1	(1,1)	1	(1,1)	2.585	(2,3)	2.995	(3,3)
		4	1	(1,1)	1	(1,1)	3	(3,3)	3	(3,3)
	(0.1, 1)	1	1	(1,1)	1	(1,1)	3	(3,3)	3	(3,3)
		2	1	(1,1)	1	(1,1)	3.045	(3,4)	3.05	(3,4)
		3	1	(1,1)	1	(1,1)	2.49	(2,3)	3	(3,3)
		4	1.01	(1,1)	1	(1,1)	3	(3,3)	3	(3,3)
	(0.1, 2)	1	1	(1,1)	1	(1,1)	3	(3,3)	3	(3,3)
		2	1	(1,1)	1	(1,1)	3.305	(3,4)	3.265	(3,4)
		3	1	(1,1)	1	(1,1)	2.36	(2,3)	3	(3,3)
		4	1.45	(1,2)	1.07	(1,2)	3	(3,3)	3	(3,3)

**Table 2** Results (continued) for computing  $\overline{\text{VaR}}_{0.99}$  with the ARA based on  $B = 200$  replications.

## 5 Conclusion

This paper presents two contributions to the computation of the worst Value-at-Risk for a sum of losses with given marginals in risk management.

First, we considered the homogeneous case and addressed the dual bound approach based on Embrechts et al. (2013, Proposition 4) and Wang’s approach based on Embrechts et al. (2014, Proposition 3.1) for computing worst Value-at-Risk. Although both of these approaches are mathematically “explicit”, care has to be exercised when computing worst Value-at-Risk bounds with these algorithms in practice. We identified several numerical and computational hurdles in their implementation and addressed them using the R package `qrmtools`; see also the detailed `demo(worst_VaR)`. We covered several numerical steps such as how to compute initial intervals for the root-finding procedures involved or clarified the uniqueness of the corresponding roots.

## 5 Conclusion

Still, we feel that we only barely scratch the tip of the iceberg. As the right-hand sides of Figures 3 and 4 hint at, in large dimensions (going up to the thousands) and with heavy-tailed distributions (such as a Pareto with parameter less than 1), all of the existing “explicit” mathematical formulas break down numerically to a degree that renders them close to being useless in practice. Besides this important word of warning (and hopefully encouraging word to highlight the *numerical* aspects of the problem of computing worst Value-at-Risk), it is likely that significantly more work has to be done in the direction of making such results truly applicable from a computational point of view (possibly requiring special, distribution-specific algorithms or computationally much more expensive multiple-precision floating-point arithmetic). The reader should keep in mind that there is a substantial difference between implementing a specific model (say, with  $\text{Par}(2)$  margins) where initial intervals can be guessed or chosen “sufficiently large” and the proper implementation of a result such as that of Embrechts et al. (2013, Proposition 4) in the form of a black-box algorithm; see the source code of `qrmtools` for more details and the work required to (just) partially go in this direction.

Second, we considered the general, i.e., non-homogeneous case. We first investigated the Rearrangement Algorithm presented by Embrechts et al. (2013). No doubt in some extent to its simplicity, this algorithm by now has been widely adopted by the industry (see also <https://sites.google.com/site/rearrangementalgorithm/>). Nevertheless, the original algorithm leaves questions unanswered concerning the concrete choice of two of its tuning parameters. These parameters were shown to have a substantial impact on the algorithm’s performance (thus they need to be chosen with care) and their choice remains largely unclear (even with detailed knowledge about the actual problem specification at hand).

We therefore presented an improved version of the Rearrangement Algorithm termed Adaptive Rearrangement Algorithm. The latter improves the former in that it addresses the aforementioned two tuning parameters. The first one is chosen automatically in an adaptive way (hence the name of the algorithm). The second one, the absolute error (which is used to determine convergence of the Rearrangement Algorithm), is replaced by two relative errors. Since they are relative errors, their choice is much more intuitive. Furthermore, one of the relative errors is used to determine the individual convergence of each of the lower and upper bounds for worst Value-at-Risk and the other relative error is used to control how far apart the two bounds for worst Value-at-Risk are; the original version of the Rearrangement Algorithm does not allow for such a control over the distance between the two bounds on worst Value-at-Risk.

The Adaptive Rearrangement algorithm has been implemented in both a readable pure R version and a fast C version (the latter currently being under construction) in the R package `qrmtools`, together with conservative defaults. Finally note that, as for the Rearrangement Algorithm, the theoretical convergence properties of the ARA remains an open problem.

## Acknowledgments

We would like to thank Ruodu Wang (University of Waterloo) for valuable comments on an early draft of this paper.

## References

- Bernard, C. and McLeish, D. (2015), Algorithms for Finding Copulas Minimizing Convex Functions of Sums, <http://arxiv.org/abs/1502.02130> (2015-02-24).
- Bernard, C., Rüschendorf, L., and Vanduffel, S. (2013), Value-at-Risk bounds with variance constraints, [http://papers.ssrn.com/sol3/papers.cfm?abstract\\_id=2342068](http://papers.ssrn.com/sol3/papers.cfm?abstract_id=2342068) (2015-02-20).
- Bernard, C., Denuit, M., and Vanduffel, S. (2014), Measuring Portfolio Risk under Partial Dependence Information, [http://papers.ssrn.com/sol3/papers.cfm?abstract\\_id=2406377](http://papers.ssrn.com/sol3/papers.cfm?abstract_id=2406377) (2015-02-20).
- Cossette, H., Denuit, M., and Marceau, É. (2002), Distributional bounds for functions of dependent risks, *Schweiz. Aktuarver. Mitt.* 1, 45–65.
- Denuit, M., Genest, C., and Marceau, É. (1999), Stochastic bounds on sums of dependent risks, *Insurance: Mathematics and Economics*, 25(1), 85–104.
- Embrechts, P. and Puccetti, G. (2006a), Aggregating risk capital, with an application to operational risk, *The Geneva Risk and Insurance Review*, 30(2), 71–90.
- Embrechts, P. and Puccetti, G. (2006b), Bounds for functions of dependent risks, *Finance and Stochastics*, 10(3), 341–352.
- Embrechts, P., Lindskog, F., and McNeil, A. J. (2003), Modelling Dependence with Copulas and Applications to Risk Management, *Handbook of Heavy Tailed Distributions in Finance*, ed. by S. Rachev, Elsevier, 329–384.
- Embrechts, P., Furrer, H., and Kaufmann, R. (2009), Different Kinds of Risk, *Handbook of Financial Time Series*, ed. by T. G. Andersen, R. A. Davis, J.-P. Kreiß, and T. Mikosch, Springer, 729–751.
- Embrechts, P., Puccetti, G., and Rüschendorf, L. (2013), Model uncertainty and VaR aggregation, *Journal of Banking and Finance*, 37(8), 2750–2764.
- Embrechts, P., Puccetti, G., Rüschendorf, L., Wang, R., and Beleraj, A. (2014), An academic response to Basel 3.5, *Risks*, 2(1), 25–48.
- Embrechts, P. and Hofert, M. (2013), A note on generalized inverses, *Mathematical Methods of Operations Research*, 77(3), 423–432, doi:10.1007/s00186-013-0436-7.
- Firpo, S. P. and Ridder, G. (2010), Bounds on functionals of the distribution treatment effects, tech. rep. (201), Escola de Economia de São Paulo, Getulio Vargas Foundation (Brazil).
- Haus, U.-U. (2014), Bounding stochastic dependence, complete mixability of matrices, and multidimensional bottleneck assignment problems, *arXiv preprint arXiv:1407.6475*.



## References

- Hofert, M. and McNeil, A. J. (2014), Subadditivity of Value-at-Risk for Bernoulli random variables, *Statistics & Probability Letters*.
- Makarov, G. D. (1982), Estimates for the distribution function of a sum of two random variables when the marginal distributions are fixed, *Theory of Probability & its Applications*, 26(4), 803–806.
- McNeil, A. J., Frey, R., and Embrechts, P. (2005), Quantitative Risk Management: Concepts, Techniques, Tools, Princeton University Press.
- Puccetti, G. and Rüschendorf, L. (2012), Computation of sharp bounds on the distribution of a function of dependent risks, *Journal of Computational and Applied Mathematics*, 236(7), 1833–1840.
- Rockafellar, R. T. and Wets, R. J.-B. (1998), Variational Analysis, Springer.
- Rüschendorf, L. (1982), Random variables with maximum sums, *Advances in Applied Probability*, 18, 623–632.
- Rüschendorf, L (1983a), On the multidimensional assignment problem, *Methods of OR*, 47, 107–113.
- Rüschendorf, L (1983b), Solution of a statistical optimization problem by rearrangement methods, *Metrika*, 30(1), 55–61.
- Williamson, R. C. and Downs, T. (1990), Probabilistic arithmetic. I. Numerical methods for calculating convolutions and dependency bounds, *International Journal of Approximate Reasoning*, 4(2), 89–158.